ELSEVIER

Thermochimica Acta 373 (2001) 97–124

thermochimica acta

www.elsevier.com/locate/tca

Review

The physical approach to the interpretation of the kinetics and mechanisms of thermal decomposition of solids: the state of the art

Boris V. L'vov*

Department of Analytical Chemistry, St. Petersburg State Technical University, Politechnicheskaya ul. 29, St. Petersburg 195251, Russia

Received 1 February 2001; received in revised form 8 March 2001; accepted 12 March 2001

Abstract

The first part of this review is devoted to a substantiation of the physical approach to the interpretation of the exponential dependence of the rate of heterogeneous reactions on temperature proposed by Hertz and Langmuir and developed by the author as an alternative to the traditional chemical approach based on the Arrhenius concept of the activation effect. The second and third parts of this work are devoted to the application of this approach to the quantitative interpretation of some important features of crystolysis reactions and identification of decomposition mechanisms for several classes of solids. The features of considered crystolysis reactions are the following: the mechanism of nucleation and autocatalytic development of decomposition reactions, the retardation of decomposition in the presence of gaseous products, the low vaporization coefficients α_v for many substances, the effect of self-cooling on the measurement of kinetic parameters, the Topley–Smith effect and the kinetic compensation effect. The physical approach has been successfully applied to the interpretation of kinetics of sublimation/dissociative evaporation of more than 110 substances from 20 different classes of solids: metals, non-metals, oxides, hydroxides, sulfides, selenides, tellurides, nitrides, azides, carbides, borides, fluorides, chlorides, bromides, iodides, carbonates, nitrates, sulfates, oxalates and hydrates. As examples of unusual results obtained, two types of reaction mechanisms should be noted: the mechanism of low-temperature (<1000°C) 'carbothermal reduction' of Fe, Co, Ni and Cu oxides and the desorption mechanism of release of sub-nanogram masses of analytes from graphite and metal surfaces. In the course of substantiation and application of the physical approach, the results obtained by different techniques (quadrupole mass spectroscopy, electrothermal atomic absorption spectrometry (ET AAS), Knudsen effusion and Langmuir free-evaporation experiments and the traditional thermal analysis) were used.

Keywords: Physical approach; Kinetics; Mechanisms; Decomposition; Crystolysis reactions

1. Introduction

> According to Sir Alan Walsh, the father of AAS: It appears to be true that 'having an idea' is not necessarily the result of some great mental leap: it is often the result of merely being able, for one sublime moment, to avoid being stupid.

There are two fundamentally different approaches to the interpretation of the exponential dependence of the rate of thermal decomposition of solids (crystolysis reactions) on temperature. The first of them is based on the Arrhenius original hypothesis that the reaction involves only an 'active part' of all reactant molecules which, according to the Maxwell–Boltzmann distribution law, is an exponential function of temperature. The second approach is based on the Hertz–Langmuir prediction of the proportional dependence of

* Tel.: +7-812-552-7741; fax: +7-812-247-4384.
E-mail address: blvov@robotek.ru (B.V. L'vov).

0040-6031/01/$ – see front matter
PII: S0040-6031(01)00507-X

the evaporation rate on the equilibrium partial pressure of the vapor which, in its turn, depends exponentially on temperature. For simplicity, the first approach will be called in the following (rather arbitrarily) as the chemical approach and the second, as the physical approach.

It is common knowledge [1–3] that the chemical approach has been transferred to the theory of crystolysis reactions from the kinetics of homogeneous reactions without appropriate theoretical validation. As a result, the kinetic parameters in the Arrhenius equation (A and E) have lost their original physical meaning. As noted by Garn [4], no discrete activated states can exist during the decomposition of a solid. Energy transfer through vibrational interactions occurs in crystals so fast that no substantial deviations from the average energy can take place. Additionally, in the case of decomposition of a solid, no collisions of freely moving reactant molecules (defined the frequency factor in the case of homogeneous reactions) can exist. Attempts to applying the simple Polanyi–Wigner equation and subsequently transition-state (or activated-complex) theory to heterogeneous reactions in the framework of Eyring–Evans–Polanyi treatments have not progressed beyond very approximate estimations of the pre-exponential factor (10^{14}–10^{16} s^{-1} [5]). In fact, the value of the pre-exponential factor is beyond these limits and in many cases becomes larger than 10^{20} s^{-1} or lower than 10^{10} s^{-1} [6].

Moreover, in the framework of chemical approach, the main features of crystolysis reactions, such as the mechanism of nucleation and the source of energy supporting the autocatalytic development of decomposition reactions, the retardation of decomposition in the presence of gaseous products, the low vaporization coefficients α_v for many substances, the effect of self-cooling on the measurement of kinetic parameters, the Topley–Smith effect and the kinetic compensation effect, remain unsolved. It is generally agreed that "this research area lacks a general theoretical framework" and "there is evidence of stagnation in the field" [7].

In the development of the physical approach and its application to the kinetics of solid-state reactions, it is possible to define (rather arbitrarily) three different periods.

1. The classical works by Hertz [8,9] in 1882 and by Langmuir [10–12] in 1913–1918 on the application of this approach to the evaporation of metals.
2. The attempts to apply this approach to the kinetics of dissociative evaporation of some simple (binary) inorganic compounds in the 1960–1980s by a research group of the University of California (mainly under the leadership of Somorjai [13] and Searcy [14,15]).
3. The development of this approach over the last two decades by L'vov [16–21] as applied to all types of solids, including crystolysis reactions with the formation of solid products.

The surprising thing is that despite the relatively earlier development of the physical approach [8,9] in comparison with that of chemical approach [22] and in spite of the much more similar features of heterogeneous crystolysis reactions and the evaporation process (the simplest heterogeneous reaction) in comparison with homogeneous reactions in the liquid and gas media, the physical approach has been completely ignored by all the workers in the field of traditional thermal analysis for the interpretation of crystolysis kinetics and, in particular, the exponential dependence of the decomposition rate on temperature. It may be supposed that this indifference is partly connected with the absence (or lack) in the literature of the systematic presentation of the foundations of the physical approach and its fundamental distinction from the chemical approach.

The objectives of this review are to discuss the basics of the theory of the physical approach more thoroughly than was done earlier and to summarize the results of its application to the quantitative interpretation of the features of crystolysis reactions enumerated above and elucidation of decomposition mechanisms of several important classes of solids by comparing experimental and theoretical values of kinetic parameters.

2. Theoretical

2.1. Basic assumptions (postulates)

The basic assumptions underlying the physical approach in most recent presentation may be formulated as follows.

1. The primary step of decomposition consists of the congruent dissociative evaporation of reactant.
2. Primary decomposition products may differ of those at equilibrium.
3. Vaporized molecules reach complete equilibration with the condensed phase upon every collision.
4. The energy evolved in the process of condensation of low-volatility product in the reaction interface is approximately equally divided between the reactant and product phases with the direct consumption of this energy by the reactant for the decomposition (as a part of the enthalpy change).

Of these postulates, assumptions (2) and (3) are rather common and obvious and there is little sense in proving their validity. In contrast, assumptions (1) and (4) might appear at first sight unreliable or at least very unusual. We should dwell on these postulates in more detail.

The assumption of the congruent dissociative evaporation of reactant as the primary step of decomposition, irrespective the low volatility of one of the products (usually, metal or metal oxide), was generated in our studies of the mechanism of carbothermal reduction of oxides [23] as a result of logical (purely mental) speculations. Let us assume for a moment that in the process of thermal decomposition of Ag_2O, the atoms of silver (residual product) do indeed avoid somehow the stage of primary gasification and remain in their original positions determined by the oxide crystal lattice. But how, pray, would they learn 'in advance' about their fate in contrast, for instance, to atoms of Zn or Cd, which transfer to the gas phase [23] in the process of decomposition of ZnO and CdO? Would is not be simpler to assume that they do not 'know' this and enter the condensed product phase later as a result of collisions with one another?

These arguments later received strong experimental support from direct quadropole mass spectrometric (QMS) observations of the primary gaseous products in the processes of thermal decompositions of microgram masses of several metal nitrates. The experimental conditions and results of these studies [24–33] are summarized in Table 1. Two different techniques were used. In vacuum experiments, a small graphite heater with a sample of metal nitrate was installed inside the vacuum chamber of the QMS (Fig. 1A). In 1 atm N_2 experiments, a flow of nitrogen from a heated graphite tube, containing a sample, was introduced into QMS through a small orifice in the sample cone (Fig. 1B). As can be seen from Table 1, the appearance of low-volatility metal species for Ag, Cd, Co, Cr, Cu, Ni, Pb, Mg, Ca, Sr and Ba nitrates was observed at temperatures in the range 340–625 K. It must be emphasized that in the cases of samples heated to

Table 1
Mass-spectrometric observations of the low-volatility species in the process of thermal decomposition of some metal nitrates

Reactant	Environment	Analyte mass (μg)	Heating rate ($K\,s^{-1}$)	Metal species		T_{app} (K)	Reference
				Major	Minor		
$AgNO_3$	Vacuum	10	1	Ag	$AgNO_3$	580	[32]
$Cd(NO_3)_2$	Vacuum	0.26	300	$CdNO_3$	Cd	550	[29]
$Cd(NO_3)_2$	Vacuum	10	1	$CdNO_3$	CdO, Cd	570	[32]
$Co(NO_3)_2{\cdot}6H_2O$	Vacuum	0.5	500	CoO		400	[27]
$Cr(NO_3)_3$	Vacuum	0.15	780	CrO	Cr_2O_3, Cr	400	[31]
$Cu(NO_3)_2{\cdot}3H_2O$	Vacuum	1	200	CuO	Cu	340	[28]
$Cu(NO_3)_2{\cdot}3H_2O$	Vacuum	10	1	$Cu(NO_3)_2$	CuO, Cu	350	[33]
$Ni(NO_3)_2{\cdot}6H_2O$	Vacuum	0.5	500	NiO		625	[26]
$Pb(NO_3)_2$	Vacuum	0.15	1000	PbO	Pb	550	[24]
$Pb(NO_3)_2$	Vacuum	0.4	600	PbO	Pb	550	[24]
$Pb(NO_3)_2$	Vacuum	10	1	$PbNO_3$	PbO, Pb	530	[32]
$Mg(NO_3)_2{\cdot}6H_2O$	1 atm N_2	0.05	2000	$Mg(OH)_2$	MgO	400	[30]
$Ca(NO_3)_2{\cdot}4H_2O$	1 atm N_2	0.05	2000	$Ca(OH)_2$		610	[30]
$Sr(NO_3)_2{\cdot}4H_2O$	1 atm N_2	0.05	2000	$Sr(OH)_2$		400	[30]
$Ba(NO_3)_2$	1 atm N_2	0.09	2000	$Ba(OH)_2$	BaO	400	[30]

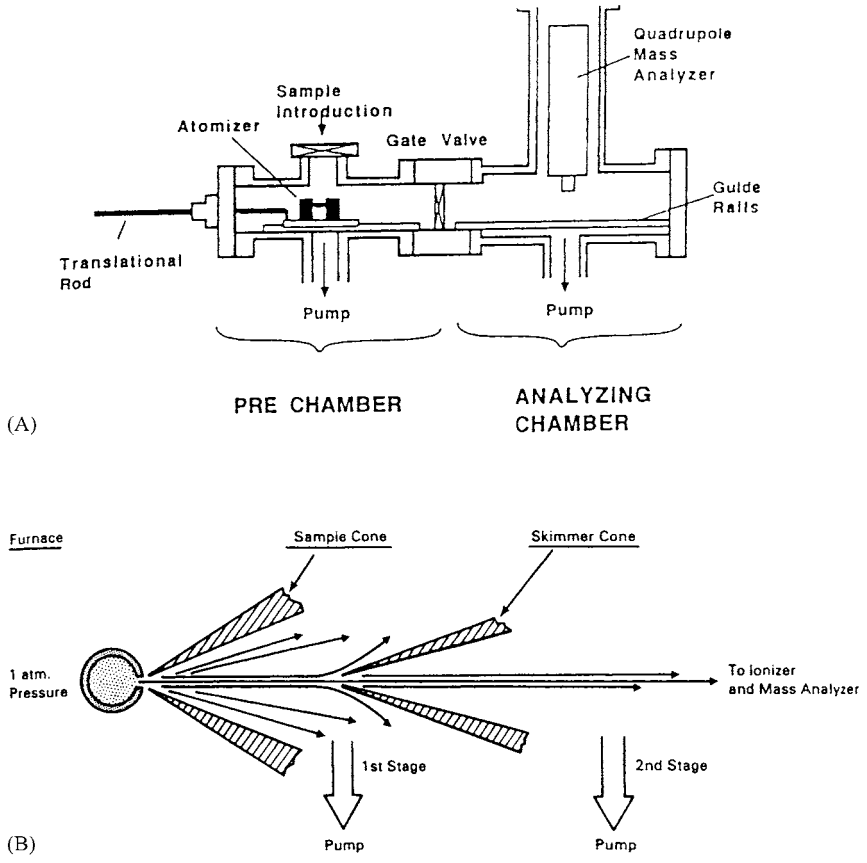

Fig. 1. (A) Schematic representation [25] of the one-stage vacuum pumping system with loading chamber. The atomizer and furnace support are shown in the loading position. (B) Schematic representation [34] of the nested-pair of cones used for sampling and molecular beam formation. Species entering the sampling cone are entrained in a free-jet expansion into vacuum stage (5×10^{-3} Pa). Only those species having momenta directed along the cone axis enter the skimmer cone.

their complete evaporation, two peaks were observed. The low- and high-temperature peaks correspond, respectively, to the decomposition of nitrate and oxide (CdO, Cr_2O_3, CuO, NiO and PbO). As an illustration, the signals of gaseous species in the process of $Ni(NO_3)_2$ and $Pb(NO_3)_2$ decomposition are reproduced in Fig. 2A and B. The area of both (low- and high-temperature) peaks for all nitrates was about the same. This means that the decompositions of nitrates occurred congruently and half of metal vapors, as expected, condensed on the surface of graphite heater. Though all known QMS investigations were performed only with metal nitrates (these compounds are of primary interest in electrothermal atomic absorption spectrometry (ET AAS)), it may be concluded that the congruent evaporation of reactant as a primary stage of decomposition is a common feature of all crystolysis reactions.

The first part of assumption (4) concerning the equipartition of condensation energy (of the low-volatility product) between the reactant and product in the reaction interface seems to be rather obvious, if both phases are at the same temperature. More difficult to prove is the validity of the second part of this assumption concerning the direct consumption of this energy by the reactant for the decomposition (as a part of the enthalpy change). Unfortunately, the mechanism of energy transfer on crystals (and the mechanism of the energy dissipation) in the process of collisions of molecules with crystalline surfaces is not clear.

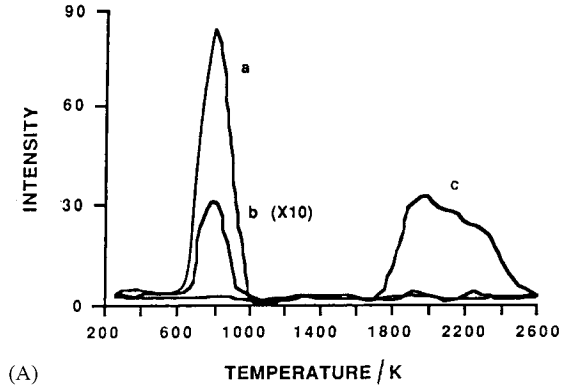

(A)

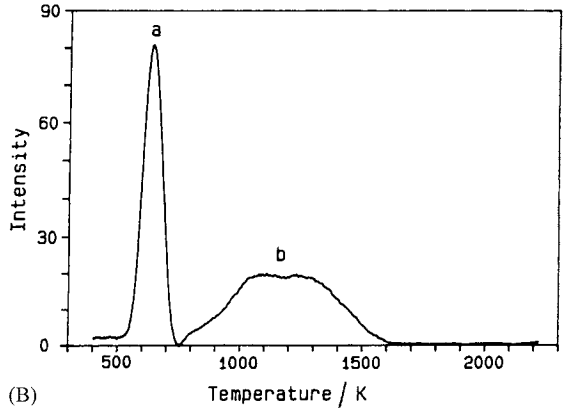

(B)

Fig. 2. (A) Mass intensity signals of Ni-species for the thermal decomposition of nickel nitrate sample containing 0.5 μg Ni: (a) NiO^+; (b) $Ni(NO_3)_2{}^+$ and (c) Ni^+ [26]. (B) Mass intensity signals of Pb-species for the thermal decomposition of lead nitrate sample containing 0.4 μg Pb: (a) PbO^+ and (b) Pb^+ [25].

There are only a few theoretical and experimental studies in this field [35]. We may only speculate that at decomposition temperature the crystalline surface of reactant is in a very unstable pre-dissociation state and any additional transfer of energy to the lattice should terminate in failure. Thus, the validity of this postulate can be checked only indirectly. The available evidence (material) will be discussed later (see Section 4.3.4).

2.2. Models

2.2.1. Evaporation rate

In 1882 Hertz (being only 25-year-old) published his, now 'classic', work [8,9] describing results of the study on the evaporation of mercury in vacuum and comparison of experimental results with theory. Probably, Hertz suspected that it is impossible to calculate the evaporation rate of direct process theoretically (the experience accumulated over more than 100 years has elapsed since Hertz proved this) and, instead of this, he proposed to calculate the maximum rate of condensation (Fig. 3). Theoretical analysis of these experiments by Hertz led to two fundamental conclusions: first, every substance has a maximum rate of evaporation which is dependent only upon the surface temperature and the properties of the substance and second, the maximum rate of evaporation cannot exceed the rate of the reverse process, namely, condensation, occurring under equilibrium conditions.

The rate of this reverse process can be easily calculated on the basis of kinetic theory of gases. It is determined by the number of molecules from the vapor phase that are incident upon the surface of the condensate:

$$J = \frac{C_{eq}\overline{u}}{4} \tag{1}$$

where C_{eq} is the equilibrium concentration of molecules per unit volume, and $\overline{u}$ the mean velocity of molecules with molar mass M:

$$\overline{u} = \left(\frac{8RT}{\pi M}\right)^{1/2} \tag{2}$$

where R is the gas constant and T the absolute temperature. The equilibrium concentration of molecules can be expressed in terms of the equilibrium pressure through the Clapeyron–Mendeleev equation:

$$C_{eq} = \frac{N_A P_{eq}}{RT} \tag{3}$$

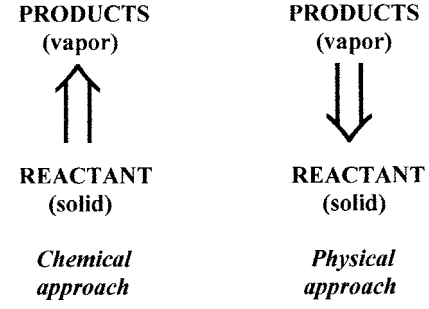

Fig. 3. The fundamental difference between two approaches in modeling of evaporation process.

where N_A is the Avogadro number. Substituting Eqs. (2) and (3) into Eq. (1) yields

$$J = \frac{N_A P_{eq}}{(2\pi MRT)^{1/2}} \tag{4}$$

This relationship derived as shown here by Langmuir [10] is usually called the Hertz–Langmuir equation.

If a foreign gas is present, the vaporization rate is limited by the diffusion of molecules from the near-surface boundary layer. The thickness of this layer is approximately equal to the mean free path of the molecules. The molecule concentration in the boundary layer is equal to the thermodynamic equilibrium value. These concepts were validated by the methods of statistical mechanics. Recalling Fick's first law for one-dimensional diffusion and the Clapeyron–Mendeleev equation, we find for the flux of molecules:

$$J = \frac{C_{eq} D}{z} = \frac{N_A D P_{eq}}{zRT} \tag{5}$$

where D is the coefficient of diffusion and z the distance from the vaporization surface to the sink, where the molecule concentration drops to zero. This relationship is called the Langmuir one-dimensional diffusion equation [12]. In the case of spherical particles of radius r_0, Eq. (5) may be presented in the form [12]

$$J = \frac{N_A D P_{eq}}{r_0 RT} \tag{6}$$

In the case of a monolayer distribution of sample, the rate constant is as follows:

$$k = \frac{J}{q} \tag{7}$$

where q is the surface density or, in other words, the number of vaporizing particles (atoms or molecules) per unit of surface area of the substance. The q value can be estimated from the formula

$$q = \left(\frac{N_A \rho}{M_r}\right)^{2/3} \tag{8}$$

where ρ and M_r are the density and molar mass of the substance (reactant). In the case of evaporation of spherical particles of radius r_0 [36]

$$k = \frac{J M_r}{N_A \rho r_0} \tag{9}$$

In the limit, when the particle radius is reduced to several ångströms ($n \times 10^{-10}$ m), Eqs. (7) and (9) approximate to the same relationship between J and k values.

2.2.2. Equilibrium pressure of product for dissociative evaporation

In the case of a compound S decomposed into gaseous products A, B and C, i.e.

$$S(s) \rightarrow aA(g) + bB(g) + cC(g) \tag{10}$$

where P_A is the partial pressure of product A can be calculated from the equilibrium constant, K_P, for reaction (10). In the absence of reaction products in the reactor atmosphere, the situation corresponding to the *equimolar* evaporation mode, the partial pressure P_A can be expressed [20] as

$$\begin{aligned} P_A^e &= a\left(\frac{K_P}{F}\right)^{1/v}\left(\frac{M_A}{M_B}\right)^{b/2v}\left(\frac{M_A}{M_C}\right)^{c/2v} \\ &= \frac{a}{F^{1/v}}\left(\frac{M_A}{M_B}\right)^{b/2v} \\ &\quad \times \left(\frac{M_A}{M_C}\right)^{c/2v} \exp\frac{\Delta S_T^\circ}{vR} \exp\left(-\frac{\Delta_r H_T^\circ}{vRT}\right) \end{aligned} \tag{11}$$

where

$$F \equiv a^a \times b^b \times c^c \tag{12}$$

$$v = a + b + c \tag{13}$$

and

$$K_P = P_A^a \times P_B^b \times P_C^c \tag{14}$$

where $\Delta_r H_T^\circ$ and ΔS_T° are, respectively, the changes of the enthalpy and entropy in reaction (10).

If the partial pressure P'_B of one of the gaseous components (B) greatly exceeds the equivalent pressure P_B of the same component released in the decomposition and if, in addition to that, the magnitude of P'_B remains constant in the process of decomposition, we call such an evaporation mode *isobaric*. In this case

$$\begin{aligned} P_A^i &= \frac{K_P^{1/(a+c)}}{(P'_B)^{b/(a+c)}}\left(\frac{M_A}{M_C}\right)^{c/2(a+c)} \\ &= \frac{1}{(P'_B)^{b/(a+c)}}\left(\frac{M_A}{M_C}\right)^{c/2(a+c)} \exp\frac{\Delta S_T^\circ}{(a+c)R} \\ &\quad \times \exp\left(-\frac{\Delta_r H_T^\circ}{(a+c)RT}\right) \end{aligned} \tag{15}$$

In order to take into account the partial transfer of the energy released in the condensation of low-volatility

product A to the reactant (see Section 2.1), we introduce into calculations of the enthalpy of decomposition reaction (10) an additional term $\tau a\,\Delta_c H^\circ_T(A)$, where the coefficient τ corresponds to the fraction of the condensation energy transferred to the reactant. Thus, we can write

$$\Delta_r H^\circ_T = a\,\Delta_f H^\circ_T(A) + b\,\Delta_f H^\circ_T(B) + c\,\Delta_f H^\circ_T(C) - \Delta_f H^\circ_T(S) + \tau a\,\Delta_c H^\circ_T(A) \quad (16)$$

The most plausible of all conceivable mechanisms for the energy transfer appears to be thermal accommodation [35] or, in other words, direct transfer of the energy at the reaction interface in collisions of the low-volatility molecules with the reactant and the product surface. For equal temperatures of the solid phases, one may expect equi-partition of energy between the two phases, i.e. $\tau = 0.5$. For the majority of substances investigated up to now, the condition $\tau = 0.5$ is found to be valid.

2.2.3. Theoretical calculation of kinetic parameters

Eqs. (6)–(15) can be used for calculation of the main parameters determining the kinetics of sublimation/decomposition of solids: the evaporation rate J, the rate constant k, the initial decomposition temperature T_{in}, and two traditional Arrhenius parameters (the pre-exponential factor, A, and the so-called activation energy, E), entering the Arrhenius equation

$$k = A\exp\left(-\frac{E}{RT}\right) \quad (17)$$

As can be seen from Eqs. (11) and (15), the E parameter for reaction (10) should be different for the equimolar and isobaric modes of decomposition, i.e.

$$E^e = \frac{\Delta_r H^\circ_T}{v} = \frac{\Delta_r H^\circ_T}{a+b+c} \quad (18)$$

for the equimolar mode and

$$E^i = \frac{\Delta_r H^\circ_T}{v-b} = \frac{\Delta_r H^\circ_T}{a+c} \quad (19)$$

for the isobaric mode. In both cases, the E parameter corresponds to the *specific enthalpy*, i.e. the enthalpy of decomposition reaction reduced to 1 mol of primary products without including components of that present in excess. The difference between the meaning of the E parameter in the framework of the chemical and the physical approaches is illustrated schematically in Fig. 4.

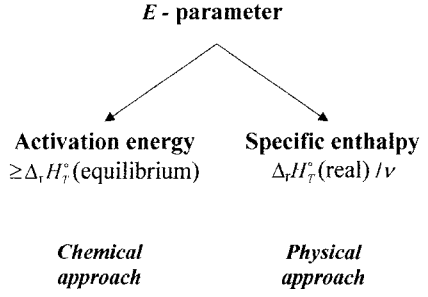

Fig. 4. Interpretation of the E parameter in different approaches. The values of $\Delta_r H^\circ_T$ (equilibrium) and $\Delta_r H^\circ_T$ (real) correspond to the enthalpies of equilibrium and real decomposition reactions, respectively. For many substances (see Section 4.2), these values are identical.

By combination of Eqs. (11) and (15) with Eqs. (4)–(9), it is easy to obtain relationships for the calculation of the A parameter. For example, in the case of decomposition of spherical particles in vacuum (the equimolar mode) in accordance with process (Eq. (10)), by combination of Eqs. (4), (9) and (11), we obtain

$$A^e = \frac{\gamma M_r}{\rho r_0 (2\pi M_A RT)^{1/2}} \frac{a}{F^{1/v}} \left(\frac{M_A}{M_B}\right)^{b/2v} \times \left(\frac{M_A}{M_C}\right)^{c/2v} \exp\frac{\Delta S^\circ_T}{vR} \quad (20)$$

In the case of decomposition of spherical particles in the presence of excess of the gaseous component B (the isobaric mode), by combination of Eqs. (4), (9) and (15), we obtain

$$A^i = \frac{\gamma M_r}{\rho r_0 (2\pi M_A RT)^{1/2}} \frac{1}{(P'_B)^{b/(a+c)}} \times \left(\frac{M_A}{M_C}\right)^{c/2(a+c)} \exp\frac{\Delta S^\circ_T}{(a+c)R} \quad (21)$$

where $\gamma = 101{,}325$ Pa atm^{-1} is the conversion factor from atmospheres used to calculate partial pressures in chemical thermodynamics to pascals. The superscripts e and i denote the pre-exponential factor, A, for equimolar and isobaric modes, respectively.

Taking logarithms and solving Eq. (11) for the temperature contained in the enthalpy factor, we

obtain the following relationship for the calculation of the initial decomposition temperature:

$$T_{in} = \frac{\Delta_r H^\circ_T}{\Delta S^\circ_T + vR[\ln v - \ln F/v + (b/2v)\ln(M_A/M_B) + (c/2v)\ln(M_A/M_C) - \ln P_\Sigma]} \quad (22)$$

where $P_\Sigma \equiv (v/a)P_A$.

Neglecting the first four insignificant items in the square brackets of Eq. (22) and taking into account Eq. (18), we come to the important relationship

$$\frac{T_{in}}{E} \cong \frac{1}{\Delta S^\circ_T/v - R\,1n\,P_\Sigma} \quad (23)$$

For the theoretical estimation of initial temperatures of reduction and appropriate P_Σ values, two practically important parameters can be used: the average initial radius of reactant particles, r_0, and the total time of decomposition, t_0. Upon integration of equation

$$J = -\frac{dm}{dt}(4\pi r^2)^{-1} \quad (24)$$

and taking into account Eq. (4) valid for the decomposition in vacuum, and the obvious relationship: $m = (4/3)\pi r^3\rho$, where m, r and ρ are the mass, radius and density of reactant spherical particle(s), respectively, we obtain a simple expression

$$P_A = \frac{\rho(2\pi M_A RT)^{1/2}}{\gamma M_r}\frac{r_0}{t_0} \quad (25)$$

Substituting into Eq. (25) rather arbitrary values of parameters: $\rho = 6500$ kg m^{-3}; $T = 1000$ K; $M_A = 0.032$ kg mol^{-1} and $M_r = 0.075$ kg mol^{-1}, we obtain

$$P_A \cong 35\left(\frac{r_0}{t_0}\right) \quad (26)$$

where P_A, r_0 and t_0 are expressed in atm, m and s, respectively. Assuming, for example, $r_0 = 10\mu m = 1 \times 10^{-5}$ m and $t_0 = 1h = 3600$ s, we have $P_A \cong 1 \times 10^{-7}$ atm.

3. Quantitative interpretation of some features of crystolysis reactions

3.1. The evolution of solid-state reactions

The use of the scheme of dissociative evaporation of the reactant with simultaneous condensation of the low-volatile product has permitted us to draw some conclusions of a general nature bearing on the evolution of solid-state reactions. These are as follows.

1. The mechanism of nucleation through condensation of the supersaturated vapor of the low-volatile product becomes fairly obvious [37].
2. During the initial decomposition stage, in the absence of any nuclei on the reactant surface, which provide sites for the condensation of the vapor of the low-volatile product at the interface zone and energy transfer to the reactant, the decomposition proceeds more slowly. The time taken to form the first nuclei on the surface of the reactant corresponds to the induction period.
3. The presence of defects or foreign impurities on the surface turns out to be equivalent to the appearance of nuclei of a new phase. Because of this, the induction and the acceleratory periods, in which the product film covers the whole surface of reactant and the reaction reaches a steady state, become shorter or disappear totally.
4. One readily understands now the phenomenon of self-localization of the process, or, in other words, the confinement of the reaction surface to the zone adjoining the product nucleus, a defect or an impurity inclusion. Due to condensation energy transfer to the reactant in this zone, the decomposition proceeds more rapidly.
5. The absence of product film on the surface of the solid reactant during the initial periods of decomposition accounts for the appearance of the low-volatile products (Ag, CdO, PbO, etc.) in the gaseous phase, as it was observed in the process of decomposition of microgram amounts of nitrates [19,32,33]. This phenomenon is most pronounced if, at the decomposition temperature, the reactant is in the liquid phase and formation of such a film is unlikely. This was the case in $AgNO_3$ and $Cd(NO_3)_2$ decompositions [32].
6. The formation of a solid product through vapor condensation accounts for the perfect character of the crystalline lattice of the product.

3.2. The retardation of decomposition in the presence of gaseous product

Application of the dissociative evaporation scheme to the thermal decomposition of solid substances permitted a theoretical evaluation of the effect of external pressure of one of the gaseous products in the reactor on the E parameter, rate and temperature of decomposition. We extended the propositions, which had earlier been theoretically formulated and experimentally confirmed for the simpler thermal decomposition reactions considered in ET AAS, involving formation of only gaseous products [16,17,20], to the decomposition of solid substances involving formation of solid products. This relates, firstly, to consideration of the two typical modes of decomposition, namely, equimolar (in the absence of primary products in the reactor) and isobaric (in the presence of one of the primary products in excess in the reactor), with the E parameters differing by $(v - b)/v$ times, and, secondly, to the inverse dependence of the decomposition rate k (or of flux J) on $(P'_B)^{b/(v-b)}$. Here v is the total number of moles of primary decomposition products, b the number of moles of product B evolving from the decomposition of 1 mol of the reactant and P'_B is the external partial pressure of gaseous product B in the reactor. The constancy of the product $(P'_B)^{b/(v-b)} \times k$ under variation of P'_B is demonstrated convincingly by the experimental data of Criado et al. [38] describing the thermal decomposition of $CaCO_3$ in the presence of CO_2 (Table 2).

To illustrate the validity of these principles for any decomposition reaction, Figs. 5 and 6 display Arrhenius plots for dehydration of $CaC_2O_4{\cdot}H_2O$ and $La_2(CO_3)_3{\cdot}8H_2O$. In both cases, we observe two regions in the Arrhenius plots: isobaric and equimolar, at lower and higher temperatures, respectively. The slopes of the Arrhenius plot in these regions are in close agreement with the theoretical predictions: the ratio of E parameters, E^i/E^e, is equal to 1.9 [39] instead of the expected 2, for $CaC_2O_4{\cdot}H_2O$ and to 8 [40], instead of the expected 9, for $La_2(CO_3)_3{\cdot}8H_2O$. Table 3 presents the corresponding data for these and some other hydrates.

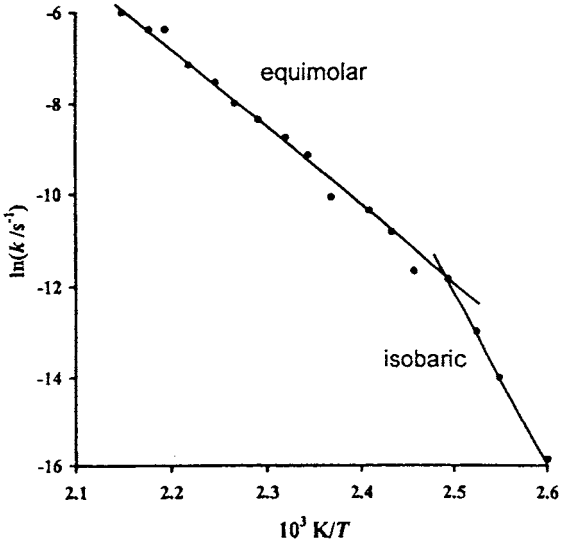

Fig. 5. Arrhenius plot for the dehydration of $CaC_2O_4{\cdot}H_2O$ under an atmosphere of air (reproduced from Dollimore et al. [39]).

The same pattern of the effect of external partial pressure of a gaseous product on the kinetic parameters observed in decomposition processes involving the formation of only gaseous products and partial formation of solid products strongly supports (sic) the assumption of the dissociative evaporation of reactant as a primary step for any decomposition reaction (see Section 2.1).

The depressing effect exerted on the decomposition rate by one of the assumed products introduced into the reactor in an excess amount may be used as an

Table 2
The kinetic parameters of $CaCO_3$ decomposition at different pressures of CO_2 [38][a]

P_{CO_2} (kPa)	E (kJ mol^{-1})	ln (A min^{-1})	k at 1000 K (min^{-1})	$P_{CO_2} \times k$ (kPa min^{-1})
1.33	187	21.2	0.275	0.37
2.67	196	21.6	0.139	0.37
12.0	188	18.8	0.0221	0.27
20.0	195	19.7	0.0234	0.47

[a] Non-isothermal experiments were performed at a heating rate of 12 K min^{-1}. Sample mass was about 25 mg [38].

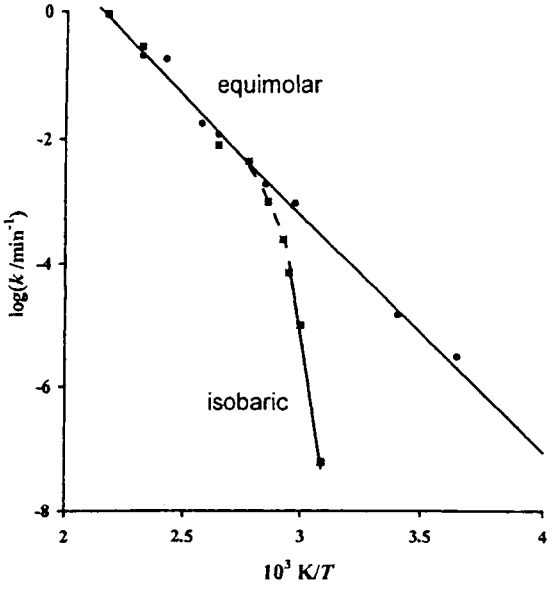

Fig. 6. Arrhenius plot for the dehydration of $La_2(CO_3)_3{\cdot}8H_2O$ in vacuum (●) and under 10 Torr of water vapor (■) (reproduced from Pavlyuchenko et al. [40]).

additional criterion for correct selection of the primary-product composition. Indeed, this results in a change not only of the decomposition mode and, hence, of the E parameter (see Section 2.2), but also of the rate and temperature of decomposition. Therefore, a significant change in one of these parameters in the presence of a potential reaction product is a reliable indication of its correct identification.

We used this criterion for the identification of the products of decomposition of ZnO [45] and then, of HgO [46]. Recently, the same criterion has been used for the identification of the composition of primary products of decomposition of oxalates [47]. In Table 4 we summarize some of these results for $Ag_2C_2O_4$ and HgC_2O_4. Experimental values of the retardation factor for $Ag_2C_2O_4$ correspond to the ratio of its decomposition rate in inert (N_2) atmosphere to that in air [48] or to that in oxygen [49] or, finally, to that in CO_2 [49]. The experimental value of the retardation factor for HgC_2O_4 corresponds to the ratio of its decomposition rate in vacuum to that in the presence of Hg vapor [50]. As can be seen from Table 4, calculations are in very satisfactory agreement with experiment. This factor is very sensitive to the composition of the gaseous products. For the decomposition of $Ag_2C_2O_4$ into $2Ag(g) + 2CO_2$, the retardation factor at 457 K in an atmosphere of CO_2 would be equal to 10^4 instead of 15 (as listed in Table 4). For the decomposition of HgC_2O_4 into $Hg(g) + 2CO_2$, the retardation factor would be equal to 130 instead of 30.

3.3. The low vaporization coefficients α_v

By the coefficient of decomposition (or vaporization in the case of the sublimation of simple substances), α_v, one usually refers to the ratio of the real gaseous-product flux, J, to the flux, J_{max}, from the effusion cell, wherein the decomposition products are expected to attain their equilibrium partial pressures. Judging from numerous experimental measurements, $\alpha_v \ll 1$ for many substances, i.e. they decompose more slowly than expected based on effusion-cell experiments. This discrepancy is usually attributed to the multi-stage character of the evaporation process, specific features of surface relief and impurities and lattice defects of the reactant [13,14,37].

L'vov and Novichikhin [45] explained this effect as due to the difference between the true scheme of thermal decomposition of a given compound and

Table 3
Dehydrations of some hydrates in different modes

Hydrate	ΔT (K)	E (kJ mol^{-1})		v	E^i/E^e	Reference
		Isobaric	Equimolar			
$CaC_2O_4{\cdot}H_2O$	382–465	281	147	2	1.9	[39]
$Cu(CH_3COO)_2{\cdot}H_2O$	353–406	154	76	2	2.0	[41]
$MnHPO_4{\cdot}3H_2O$	303–375	251	57	4	4.4	[42]
$Y_2(CO_3)_3{\cdot}4H_2O$	298–453	154	35	5	4.4	[43]
$Na_3P_3O_9{\cdot}6H_2O$	260–308	264	41	7	6.4	[44]
$La_2(CO_3)_3{\cdot}8H_2O$	270–430	515	65	9	7.9	[40]

Table 4
Retardation of oxalate decomposition in the presence of gaseous product (B)

Oxalate	T (K)	P'_B (atm)	Primary products	Retardation factor		Reference
				Calculated	Experimental	
$Ag_2C_2O_4$	404	0.21 (O_2)	$2Ag(g) + CO + CO_2 + 0.5O_2$	5	4	[48]
	457	1.0 (O_2)		4	2	[49]
	457	1.0 (CO_2)		15	9	[49]
HgC_2O_4	463	0.017 (Hg)	$Hg(g) + CO + CO_2 + O$	30	25	[50]

one which assumes direct decomposition to the final products in thermodynamic equilibrium (as is the case in the effusion cell). These differences consist, first, in primary gasification of all decomposition products, including low-volatility components (metals and metal oxides) and, second, in the partial or total evolution of gaseous species in a form different from the equilibrium composition. By properly choosing the primary-product composition, we have succeeded in interpreting the low values of α_v for a large group of inorganic compounds and some non-metals [45]. These data will be considered below in Section 4.3 and, anticipating these results, it is possible to note that the lowest values of α_v (in the range of 10^{-17} to 10^{-40}) correspond to azides and oxalates. These compounds are explosives. Nevertheless, because they decompose into primary products very different from equilibrium products, they are rather stable at room temperature.

3.4. The effect of self-cooling on the measurement of kinetic parameters

Most studies of the decompositions of powders and single crystals in thermal analysis tacitly assume that the temperature of the sample is equal to that of the furnace, and that the self-cooling due to some heat being expended in the endothermic decomposition can be neglected. However, as early as 1931, Smith and Topley [51] showed that the temperature of a single crystal in vacuum was lower than that in the furnace by 4–8 K. It is rather obvious that, for powders, the self-cooling effect should be much greater.

L'vov et al. [52,53] proposed a fairly simple theoretical model and developed a program to compute the temperature of individual crystals and the layer-by-layer temperature distribution in powder samples during the course of their decomposition in vacuum and in the presence of foreign gases. Simulation of the temperature distribution, inside a powder sample, can be reduced to modeling the vertical distribution between horizontal layers of this material of thickness equal to the powder grain diameter. If the furnace temperature is the same on top and at the bottom of the sample, the analysis can be limited to considering only one half of such multilayered sample, from the central, zeroth or first layer, to the nth outermost layer. All the calculations were performed with the laboratory-developed computer program described in [53].

The results of the calculations performed for fairly typical conditions of thermal decomposition of $Mg(OH)_2$ in vacuum [52] and $Li_2SO_4{\cdot}H_2O$ in the presence of foreign gases [53] enabled the following conclusions to be drawn.

1. For moderate decomposition rates, the temperature difference between the hottest (surface) and the coldest (central) layer of a powder may be as high as tens and even hundreds of degrees, depending on the total number of layers, n. As an illustration, see Fig. 7. For instance, for $n = 1000$ and 10,000, the temperature of the central layer of a $Mg(OH)_2$ sample decomposing in vacuum, irrespective of the furnace temperature (500 or 600 K), is only 427 and 387 K, respectively.
2. Even for single crystals, particularly for their decomposition in vacuum, the temperature of the surface can differ significantly from that of the furnace. For instance, for furnace temperatures of 550, 600 and 663 K, the temperature of single-crystal $Mg(OH)_2$ is expected to be 549.6, 593 and 628 K, respectively.

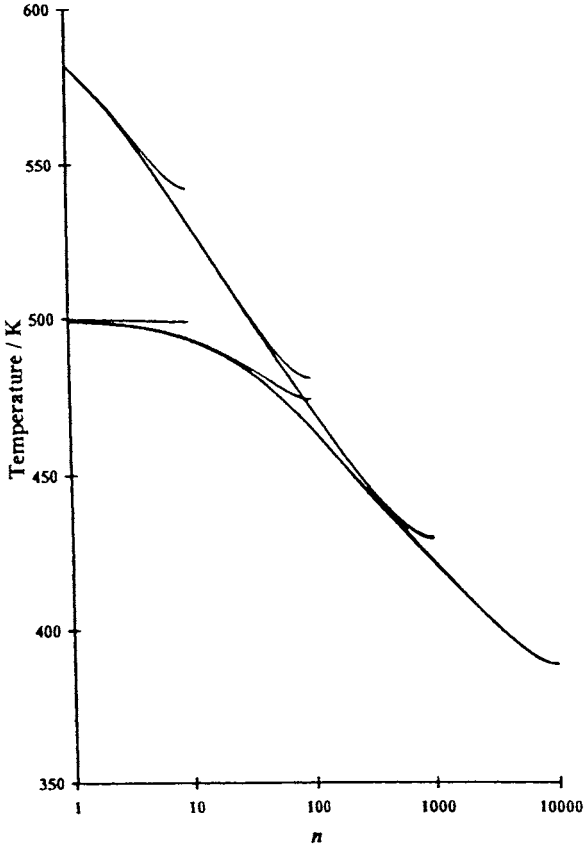

Fig. 7. Calculated [52] temperature distribution for a $Mg(OH)_2$ powder in vacuum at 500 and 600 K furnace temperature for the following different numbers of layers: 10, 10^2, 10^3 and 10^4.

These results cast doubt on the correctness of many kinetic measurements performed with powder samples, particularly in vacuum. This relates to the measurements of both decomposition rates and E parameters. Given the temperature distribution in a sample, one can correct the measured kinetic parameters (k, J, and E) for the self-cooling effect [52]. This is naturally much simpler and more reliable to do for single crystals than for powder samples. In the latter case, in order to find the number of layers, n, one must know the average size of grains and their number in the sample, as well as the crucible geometry. This was done to calculate the corrections to measured absolute decomposition rates and E parameters in the case of dehydration of $Mg(OH)_2$ in vacuum [52]. Introduction of these corrections permits one to explain the differences between the kinetic parameters obtained under different conditions.

Modeling the temperature distribution made it possible for the first time to quantitatively describe some unusual effects observed during the thermal decomposition of powders. Among them is the inverse proportionality between decomposition rate and the mass of a powder sample, which at first sight appears hard to understand. If, however, one takes into account self-cooling, this relation appears obvious. Indeed, irrespective of the total number of layers, n, i.e. of the powder mass, the effective number of layers, n_e, whose decomposition proceeds at the rate of the surface layer, remains practically constant [52].

3.5. The Topley–Smith effect

Computer simulation of the Topley–Smith effect is another example of successful application of this model [53]. This effect reports essentially on the anomalous behavior of the dehydration rate of many crystalline hydrates with increasing partial pressure of water vapor in the reactor. In contrast to the expected monotone decrease of the rate with increasing P_w, the dehydration rate, on reaching a certain critical pressure (0.1–10 Torr), begins to grow, passes through a maximum, and falls off again. A theoretical calculation of the shape of $J = f(P_w)$ curve showed that this anomaly is actually the result of competition between the depressing influence of water vapor during dehydration, on the one hand, and the increasing heat transfer from the furnace to the sample by water vapor, on the other, in the presence of intense self-cooling. The model developed [53] accounted for all the main features of the Topley–Smith effect, in particular, the enhancement of the effect with increasing decomposition temperature and with decreasing powder grain size. As an illustration, Fig. 8 displays the calculated dependence of decomposition rate of $Li_2SO_4{\cdot}H_2O$ powder on partial pressure of water at different temperatures [53].

3.6. The kinetic compensation effect

As defined by Galwey and Brown ([2], p. 130), 'compensation' refers to the behavior pattern in which a rise in E (which will decrease the rate of a reaction at any particular temperature) is partially or completely

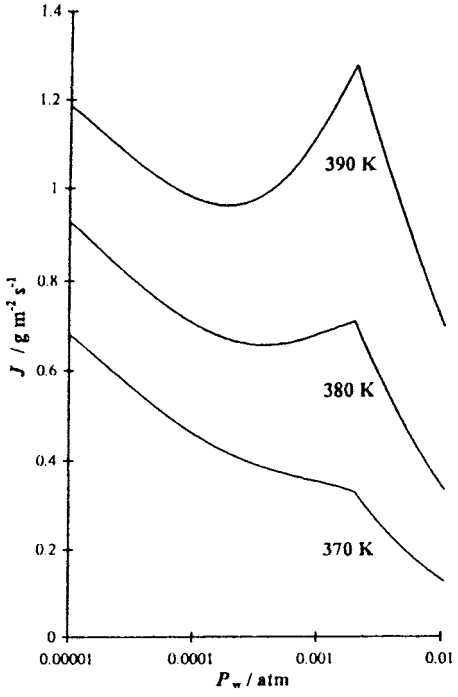

Fig. 8. Rate of decomposition of $Li_2SO_4{\cdot}H_2O$ powder as a function of partial pressure of water in a foreign-gas (air) pressure $P_a = 10^{-3}$ atm in the logarithmic P_w scale [53].

offset by an increase in A. In many cases, their variation follows the relation

$$\ln A = a + bE \tag{27}$$

where a and b are constants. After observing this effect by Zawadzki and Bretsznajder [54] in 1935 in their study of $CaCO_3$ decomposition at different CO_2 pressures, it has been a subject of much investigation. Nevertheless, "at present, no theory is accepted as explaining the compensation effect adequately" [55]. Transition-state theory used frequently for the formulation of reaction mechanisms interprets the parameters A and E as being independent. In contrast to this, in the framework of the physical approach, the presence of gaseous product in the reactor should change the values of parameters A and E in accordance with Eq. (27). As can be seen from Eqs. (18)–(21), an increase of the parameter E in the isobaric mode is accompanied by an increase of the A-parameter. The situation can be illustrated by the example of decomposition of a simple binary compound S into two products (S → A + B) in the equimolar and isobaric mode, when one of the products (A) is a low-volatility species. Taking into account Eqs. (18)–(21) and an equality of the rate constants ($\ln k^e = \ln k^i$) at the isokinetic temperature, T_θ, we can obtain (the difference in the molar masses of A and B products is neglected)

$$\frac{\Delta S^\circ_T}{2R} - \frac{\Delta_r H^\circ_T}{2RT_\theta} = -\ln P'_B + \frac{\Delta S^\circ_T}{R} - \frac{\Delta_r H^\circ_T}{RT_\theta} \tag{28}$$

On rearrangement of Eq. (28), we have

$$T_\theta = \frac{\Delta_r H^\circ_T}{\Delta S^\circ_T - 2R \ln P'_B} \tag{29}$$

In case of $P'_B = 1$ atm

$$T_\theta = \frac{\Delta_r H^\circ_T}{\Delta S^\circ_T} \tag{30}$$

Eqs. (29) and (30) can be used for the calculation of the isokinetic temperature corresponding to the different modes of decomposition. Table 5 presents the results of such calculations for the decompositions of $CaCO_3$, $Mg(OH)_2$ and $Li_2SO_4{\cdot}H_2O$ under the condition $P'_B = 1$ Torr. Experimental values of T_θ for $CaCO_3$ (1244 [55] and 1250 K [55]) and $Li_2SO_4{\cdot}H_2O$ (~400 K [55]) are very close to theory (1200 and 421 K, respectively).

Table 5
Isokinetic temperatures corresponded to the different modes of decomposition (equimolar and isobaric) under the condition $P'_B = 1$ Torr = 0.0013 atm

Reactant	Products[a]	$\Delta_r H^\circ_T$ (kJ mol^{-1})	ΔS°_T (J mol^{-1} K^{-1})	T_θ (K)
$CaCO_3$	$CaO(g)_\downarrow + CO_2$	498.2_{1200}	305.0_{1200}	1200
$Mg(OH)_2$	$MgO(g)_\downarrow + H_2O$	351.0_{600}	322.9_{600}	810
$Li_2SO_4{\cdot}H_2O$	$Li_2SO_4(g)_\downarrow + H_2O$	193.8_{298}	350.5_{298}	421

[a] Here and below, an arrow (↓) implies taking into account the condensation energy transfer to the reactant ($\tau = 0.5$ for $CaCO_3$ and 0.6 for two other reactants).

The different modes of decomposition is probably the most important reason for the scatter of reported values of the A and E parameters and manifestation of the kinetic compensation effect. In the cases, where the primary gaseous products are in the form different of those at equilibrium, for example, in the form of atoms O or N and, therefore, the isobaric mode cannot be realized (so-called 'irreversible' decompositions), different workers have reported comparable magnitudes of A and E parameters. Nevertheless, the difference in the decomposition modes is not the only reason for the scatter. Some other reasons are listed below.

1. Differences between the mathematical models used by different authors for the treatment of primary experimental data [55].
2. Effect of self-cooling of powder samples in the process of decomposition and its dependence on the particle size, mass of powder, geometry of the crucible, environmental conditions (vacuum or the presence of inert gas) and the heating rate (for non-isothermal decompositions) [52].
3. The difference in the kinetic parameters for the nucleation and steady-state stages of decomposition [47].

It should be stressed that in the framework of the physical approach, possible differences in the kinetic parameters due to last two reasons ((2) and (3)) could be theoretically calculated or at least estimated. This has been demonstrated in [47,52].

4. Identification of decomposition mechanisms

4.1. Methods of identification

There are several methods for the interpretation/identification of the mechanisms of decomposition and, in particular, their consistency with equilibrium ($\alpha_v \cong 1$). The most common is the comparative measurement of the vapor pressures of substances by Knudsen effusion and Langmuir free-evaporation techniques. In both, the experiment is carried out in a high vacuum system and the quantity of material that is transported away from the sample is measured. In the Knudsen technique, the sample is contained in an inert crucible provided with a small, thin orifice. If the orifice is sufficiently small and α_v is not very low ($>10^{-5}$–10^{-4}), equilibrium is established inside the crucible, and the rate of effusion through the orifice is fixed by the pressure of the vapor, the temperature, the molar mass of the effusion species and the dimensions of the orifice. In the Langmuir technique no crucible is used, but rather free evaporation occurs from the sample surface. This approach has been used in several laboratories, in particular, by the research groups of the Universities of California [13–15] and Chicago in the 1950–1970s. The last group used this method in combination with mass spectroscopy (see [56]).

Another check on the assumption that $\alpha_v = 1$ consists of a comparison of the vapor pressure data (as a function of temperature) with equilibrium pressure data obtained from independent experimental determinations or commonly accepted thermodynamic functions. This approach was used by Langmuir and coworkers [10,57] in investigations of evaporation rates of metals.

Some other experimental parameters describing the kinetics of solid-state reactions can be compared with the appropriate results calculated from theoretical models. In the past, this rather general approach was used to verify the validity of Polanyi–Wigner and Eyring–Evans–Polanyi theories [5]. Unfortunately, these attempts have not progressed beyond very rough estimates of the pre-exponential factor A of the Arrhenius equation. The value of the activation energy, E, was kept in the shade. Therefore, the absolute rate of reaction and its dependence on temperature remained unknown. In the majority of studies in ET AAS and classical thermal analysis, researchers attempt to understand the mechanism of release/decomposition using only the values of E parameter and ignoring the values of pre-exponential factor. The reliability of such interpretations is very low.

The physical approach to the interpretation of decomposition mechanisms differs radically from the one accepted universally. Classical thermal analysis attempts to understand the differences between the experimentally measured and theoretically predicted kinetic parameters of the decomposition process assuming the primary decomposition products have an equilibrium composition. To account for the discrepancies between calculation and experiment (most frequently, in the magnitude of E), one invokes either physical reasons (for example,

depressed diffusion of a gaseous product from the solid matrix) or some chemical steps associated with the transport of electrons, protons, positive holes, or ions among groups of atoms or ions. These explanations usually do not contain any quantitative estimates.

The physical approach is based on the assumption that the decomposition process itself reduces to congruent dissociative evaporation of the reactant, so that the kinetics of the process is determined *only* by the composition of the primary decomposition products and the experimental conditions, which govern the evaporation mode and reactant self-cooling. Thus, the search for an adequate decomposition mechanism reduces primarily to looking for a composition of primary evaporation products for which the calculated kinetic parameters are in agreement with experiment. Fig. 9 illustrates the principal differences between the universally accepted (standard) and proposed approaches.

In the identification of primary reaction products, we shall use below the E value as the main kinetic parameter which together with some of the other interrelated kinetic parameters (the pre-exponential factor, A, the rate constant, k, the flow of product species, J, the equivalent product pressure, P, the vaporization coefficient, α_v, or the initial temperature, T_{in}) completely define the kinetics of reaction. It should be stressed once again that, in accordance with the physical approach, we shall use the E value not as the energy of 'activation' (in the Arrehnius interpretation), but as the specific enthalpy of the process, $\Delta_r H^\circ_T/v$. Moreover, in some cases for the identification of gaseous species, we shall use the results of the mass spectroscopy analysis and investigation of the retardation effect in the presence of gaseous product (Section 3.2).

4.2. Solids decomposed in accordance with equilibrium ($\alpha_v \cong 1$)

There are a large number of solids which sublimate or decompose in accord with equilibrium. This means that the primary products of sublimation or decomposition for these solids correspond to the equilibrium species and the vaporization coefficient is very close to unity ($\alpha_v \cong 1$). First of all, practically all the metals can be related to them. Table 6 presents a list of metals and a few non-metals (iodine, white phosphorus and selenium) which as shown in investigations by different workers sublimate in accordance with equilibrium. Tables 7 and 8 present a list of inorganic compounds which sublimate or decompose in accord with equilibrium. Most of the compounds which sublimate at moderate temperatures (<1400 K) without any significant decomposition are the metal halides. As concluded by Brewer and Kane [70], "all elements that vaporize predominantly to atomic species, and all ionic salts such as the alkali halides that vaporize predominantly to a monomeric gaseous molecule, are believed to have vaporization coefficients close to unity". A few stable oxides (ThO_2, ZrO_2 and H_2O)

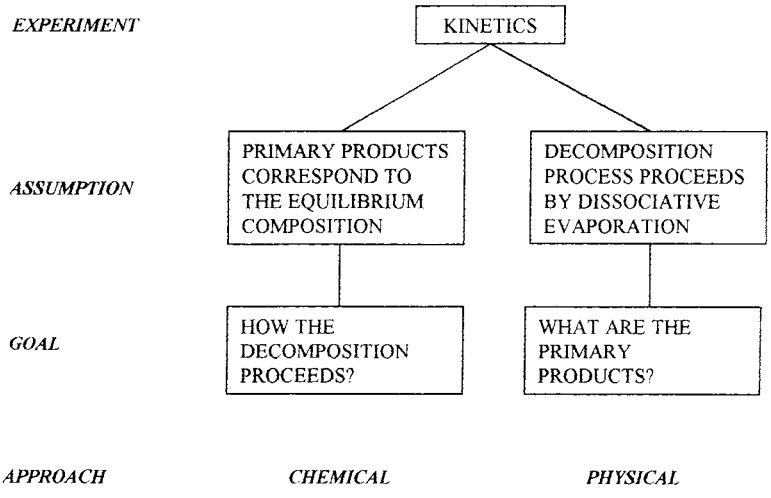

Fig. 9. Simplified schemes for the chemical and the physical approaches to the investigation of decomposition mechanisms.

Table 6
Elements sublimated in accord with equilibrium ($\alpha_v \cong 1$)

Reaction	T (K)	Reference
Ag → Ag(g)	1100	[37]
Au → Au(g)	1300	[15]
B → B(g)	2300	[15]
Be → Be(g)	1200	[37]
Cd → Cd(g)	500	[37]
Co → Co(g)	1600	[59]
Cr → Cr(g)	1300	[37]
Cu → Cu(g)	1200	[37]
Fe → Fe(g)	1500	[37]
Ge → Ge(g)	1500	[58]
Hg → Hg(g)	220	[58]
2I → I_2(g)	260	[58]
K → K(g)	350	[58]
Mo → Mo(g)	2100	[58]
Ni → Ni(g)	1400	[58]
4P (white) → P_4(g)	300	[15]
Pd → Pd(g)	1400	[60]
Pt → Pt(g)	1800	[58]
Rh → Rh(g)	2000	[60]
Ru → Ru(g)	2200	[60]
Si → Si(g)	1650	[15]
2Te → Te_2(g)	600	[58]
Ti → Ti(g)	1700	[58]
Tl → Tl(g)	550	[61]
W → W(g)	2600	[58]
Zn → Zn(g)	550	[15]

Table 7
Inorganic compounds sublimated or decomposed in accord with equilibrium ($\alpha_v \cong 1$)

Reaction	T (K)	Reference
Al_2O_3 → 2Al(g) + 3O	2300	[62]
BaF_2 → BaF_2(g)	1300	[15]
BeF_2 → BeF_2(g)	900	[63]
CaF_2 → CaF_2(g)	1400	[64]
CdO → Cd(g) + 0.5O_2	1250	[65]
CdTe → Cd(g) + 0.5Te_2	1000	[15]
$HgBr_2$ → $HgBr_2$(g)	320	[37]
$HgCl_2$ → $HgCl_2$(g)	300	[37]
HgI_2 → HgI_2(g)	350	[37]
H_2O (ice) → H_2O(g)	200	[37]
KCl → KCl(g)	800	[37]
KI → KI(g)	750	[37]
MgF_2 → MgF_2(g)	1400	[66]
LaF_3 → LaF_3(g)	1400	[15]
LiF → LiF(g)	1000	[37]
NaCl → NaCl(g)	900	[15]
PbO → Pb(g) + 0.5O_2	1000	[69]
PrF_3 → PrF_3(g)	1300	[15]
$SnCl_2$ → $SnCl_2$(g)	600	[58]
SrF_2 → SrF_2(g)	1300	[67]
ThO_2 → ThO_2(g)	2300	[68]
TiB_2 → Ti(g) + 2B(g)	2050	[68]
TiC → Ti(g) + C(g)	2400	[68]
ZrB_2 → Zr(g) + 2B(g)	2300	[68]
ZrO_2 → ZrO_2(g)	2300	[68]

are brought into this group as well. At the same time, many other oxides, as it was stated by L'vov et al. [16,17] and supported by other workers, evaporate with simultaneous dissociation into the equilibrium products: free metal atoms and O_2 molecules at $T < 2100$ K or atomic oxygen at $T > 2300$ K.

It should be noted that the theory of stepwise evaporation due to Hirth and Pound [37] predicted that most crystalline materials should evaporate into vacuum with a vaporization coefficient of $\alpha_v = 1/3$. As can be seen from the above data, this is not the case. The only example of such behavior mentioned to support this theory, was a discontinuity of the rate of evaporation of Al_2O_3 at the melting point [71]. This corresponded to $\alpha_v = 1/3$ for solid and $\alpha_v = 1$ for liquid Al_2O_3. However, several years later Paule [72] has shown that the evaporation coefficient for Al_2O_3 is constant and that the observed increase in vaporization [71] was due to an increase in the temperature which, in turn, was due to discontinuous increase in the emissivity of the melt.

Table 8
Metal oxides decomposed in accord with equilibrium ($\alpha_v \cong 1$) [20]

Reaction	T (K)	Experimental parameters[a]
Al_2O_3 → 2Al + 1.5O_2	2100	*E*, *A* (i/e-modes)
BaO → Ba + O	2400	*E*, *A* (i/e-modes)
BeO → Be + O	2300	*E*, *A* (i/e-modes)
Bi_2O_3 → 2Bi + 1.5O_2	1200	*E*, *A* (i/e-modes)
CaO → Ca + 0.5O_2	2000	*E*, *A* (i/e-modes)
CdO → Cd + 0.5O_2	800	*E*, *A* (e-mode)
Cr_2O_3 → 2Cr + 1.5O_2	2000	*E*, *A* (i/e-modes)
Ga_2O_3 → 2Ga + 1.5O_2	1500	*E*, *A* (i/e-modes)
In_2O_3 → 2In + 1.5O_2	1400	*E*, *A* (i/e-modes)
Li_2O → 2Li + 0.5O_2	1400	*E*, *A* (i/e-modes)
MgO → Mg + 0.5O_2	1700	*E*, *A* (i/e-modes)
MnO → Mn + 0.5O_2	1700	*E*, *A* (i/e-modes)
PbO → Pb + 0.5O_2	1100	*E*, *A* (i/e-modes)
Sb_2O_3 → 2Sb + 1.5O_2	1400	*E*, *A* (i-mode)
SrO → Sr + 0.5O_2	2100	*E*, *A* (i/e-modes)
V_2O_3 → 2V + 1.5O_2	2200	*E*, *A* (i/e-modes)

[a] Here i/e means both isobaric and equimolar modes.

4.3. Solids decomposed into products different of those at equilibrium

4.3.1. Preliminary comments

It follows from the experience accumulated over the last century in the field of solid-state decomposition, most of these reactions, especially for polyatomic compounds, proceed under conditions far from equilibrium [1,2]. The main concept in the traditional chemical approach consists of the belief that the deviation from equilibrium is connected with the existence of the theoretically unpredicted energy barrier (activation energy) in the way of reaction. By contrast, the main concept in the proposed physical approach consists of the belief that the only reason for this lies in the decomposition of reactant into primary gaseous species different from those at equilibrium. Therefore, the difference between the chemical and physical approaches can be reduced to a substitution of the non-equilibrium decomposition into equilibrium products to the equilibrium decomposition into non-equilibrium products.

The great advantage of the physical approach relative to the chemical model consists of the possibility for the quantitative description of the decomposition process. The main problem in this approach, however, is the correct definition of the origin and composition of these primary species.

The distinctions of primary products of decomposition from equilibrium species consist, firstly, in the primary gasification of all decomposition products, including low-volatile compounds (metals, metal oxides, metal salts, etc.), secondly, in the partial or total evolution of nitrogen, oxygen, sulfur, selenium, etc. in the form of free atoms rather than molecules, and, thirdly, in the different composition of equilibrium species (for example, in the evolution of $CO_2 + CO + 0.5O_2$ molecules instead of $2CO_2$ in the cases of Ni and Ag oxalates [47]). We shall consider below several classes of such decomposition reactions in order of their increasing complexity.

4.3.2. Solids decomposed into gaseous products different of those at equilibrium

A list of solids which decompose into gaseous products different of those at equilibrium is presented in Table 9. Together with some inorganic compounds, this includes a few non-metals: P (red), As and Sb. In addition to E used as the main parameter for identification of primary products of decomposition, one of some other kinetic parameters (P, k, J or T_{in}) was used. In some cases, additional information was obtained from the retardation effect in the presence of gaseous product, results of the direct mass spectrometry analysis of the primary species and indirect observations of atomic oxygen (based on the darkening of a platinum crucible or the blue coloration of MoO_3 during the decomposition ([2], p. 292).

The composition of the primary products for the deduced reactions in all cases corresponds to the best agreement between experimental and calculated values of both kinetic parameters: E and one of the additional P, k, J or T_{in} parameters. The discrepancy between the experiment and theory in most cases was not more than 10% for the E and T_{in} parameters and a factor of three for the P, k and J parameters.

For different solids, the vaporization coefficient α_v varies over a wide range: from 0.1 for Sb, CdS and CdSe up to 2×10^{-23} for HgC_2O_4. This difference in α_v values to a great extent depends on the initial temperature of decomposition. For example, in the cases of evolution of oxygen as atomic species, α_v is not lower than 10^{-2} at temperatures >1250 K (ZnO, $BaSO_4$, Na_2CO_3, SiO_2, GeO_2 and SnO_2) and not higher than 10^{-7} at temperatures <650 K (HgO and HgC_2O_4). It is interesting that, in contrast to the oxygen-containing compounds mentioned above, all sulfur, selenium and nitrogen-containing compounds decompose with only partial evolution of free atoms of S, Se and N. We have no explanations for this distinction.

The possibility of evolution of gaseous products in the form different of those at equilibrium has been discussed in many works in the past. As early as 1936, Melville and Gray [76] attributed the anomalously low rate of vaporization of red phosphorus to the existence of P_2 units in the solid lattice, and they hypothesized that P_2 was vaporizing with unit vaporization coefficient from the solid, but, because of the small partial pressure of P_2 compared to P_4, a very low rate of vaporization was obtained. Nesmeyanov [61] and later, Rosenblatt et al. [77] noted that arsenic has a structure closely related to the graphite structure and this means that 'tetragonal As_4 molecules do not exist as such in the metal lattice, and their formation requires considerable rearrangement of internuclear distances and angles' [77]. Margrave et al. [78]

Table 9
Thermal decomposition of substances into gaseous products different of those at equilibrium

Reactant	T (K)	Primary products		α_v	Experimental parameters[a]	Reference
		Equilibrium	Deduced			
P (red)	600	P_4	P_2	1×10^{-6}	*E*, *P*	[45]
As	550	As_4	$As_2 + As_4$	3×10^{-4}	*E*, *P*	[45]
Sb	650	Sb_4	$Sb_2 + Sb_4$	1×10^{-1}	*E*, *P*	[45]
HgO	650	$Hg + 0.5O_2$	Hg + O	8×10^{-9}	*E*, *k*, re, ind	[46]
ZnO[b]	1400	$Zn + 0.5O_2$	Zn + O	2×10^{-2}	*E*, *P*, re, ind	[45]
CdS	1000	$Cd + 0.5S_2$	$Cd + 0.3S + 0.35S_2$	1×10^{-1}	*E*, *P*, re	[45]
CdSe	1000	$Cd + 0.5Se_2$	$Cd + 0.7Se + 0.15Se_2$	1×10^{-1}	*E*, *P*	[45]
Be_3N_2	1800	$3Be + N_2$	$3Be + 1.4N + 0.3N_2$	4×10^{-3}	*E*, *P*	[45]
Mg_3N_2	1200	$3Mg + N_2$	$3Mg + N + 0.5N_2$	4×10^{-4}	*E*, *P*	[45]
AlN	1600	$Al + 0.5N_2$	$Al + 0.6N + 0.2N_2$	2×10^{-3}	*E*, *P*	[45]
GaN	1190	$Ga + 0.5N_2$	$Ga + 0.5N + 0.25N_2$	6×10^{-4}	*E*, *P*, re	[45,73]
NaN_3	600	$Na + 1.5N_2$	$Na + 0.9N + 1.05N_2$	7×10^{-13}	*E*, *J*, ms	[74]
KN_3	530	$K + 1.5N_2$	$K + 0.72N + 1.14N_2$	6×10^{-12}	*E*, *J*	[74]
$BaSO_4$	1500	$BaO + SO_2 + 0.5O_2$	$BaO + SO_2 + O$	1×10^{-2}	*E*, *P*	[21,45]
HgC_2O_4	430	$Hg + 2CO_2$	$Hg + CO + CO_2 + O$	2×10^{-23}	*E*, T_{in}, re	[47]
Na_2CO_3	1250	$2Na + CO_2 + 0.5O_2$	$2Na + CO_2 + O$	5×10^{-2}	*E*, *P*	[75]
NH_4NO_3	400	$N_2O + 2H_2O$	$NH_3 + HNO_3$	4×10^{-14}	*E*, T_{in}	[75]
SiO_2	1800	$SiO + 0.5O_2$	SiO + O	9×10^{-3}	*E*, T_{in}	[75]
GeO_2	1470	$GeO + 0.5O_2$	GeO + O	1×10^{-2}	*E*, T_{in}	[75]
SnO_2	1400	$SnO + 0.5O_2$	SnO + O	4×10^{-2}	*E*, T_{in}	[75]

[a] The re, ms and ind mean the retardation effect, mass-spectroscopy and indirect analysis, respectively.
[b] Wurtzite structure.

explained the low coefficient of vaporization of Mg_3N_2 because of the large separation of nitrogen atoms in the rigid magnesium nitride lattice. Brewer and Kane [70] generalized these observations as follows: "from the available data, low vaporization coefficients can be expected whenever the main vaporizing gaseous species are not present as such in the condensed phase and the atoms or molecules in the condensed phase are held so rigidly that they cannot readily reorganize to form the main gaseous species. It appears very unlikely that materials vaporizing predominantly to atomic gaseous species will have low vaporization coefficients". Strange, as it may seem, none of these workers tried to interpret this effect on theoretical grounds and use it for the identification of the primary products of decomposition.

4.3.3. Solids decomposed into gaseous and solid products (without taking into account the condensation energy transfer to the reactant)

During the initial periods of decomposition in the absence of a product film on the surface of the solid reactant or, alternatively, in the process of vacuum decomposition of sub-microgram masses of compounds distributed as an ultra-thin layer on the surface of a plane heater, the condensation of low-volatility species outside the reactant surface has no effect on the rate of decomposition. Therefore, the calculation of kinetics can be performed without taking into account the condensation energy transfer to the reactant ($\tau = 0$), or in the same way as it is done in the case of reactant decomposition into gaseous products only. Table 10 presents the results of such analyses in the case of the decompositions of some metal nitrates, oxalates and azides.

The absence of a product film on the surface of metal nitrates and TlN_3 is supported by the direct mass spectroscopy observations of low-volatility species in the case of nitrates and free atoms of nitrogen in the case of TlN_3. In the other cases, the only argument supporting the absence of a product film is a very low rate of decomposition at the lowest temperatures typical for these reactants. For example, the temperature of experiments for $Ba(N_3)_2$ was below 400 K,

Table 10
Thermal decomposition of inorganic compounds into gaseous and solid products ($\tau = 0$)

Reactant	T (K)	Primary products		α_v	Experimental parameters[a]	Reference
		Equilibrium	Deduced			
$AgNO_3$	600	$Ag(s) + NO_2 + 0.5O_2$	$Ag(g) + NO_2 + 0.5O_2$	1×10^{-7}	E, T_{in}, ms	[32]
$Pb(NO_3)_2$	550	$PbO(s) + 2NO_2 + 0.5O_2$	$PbO(g) + 2NO_2 + 0.5O_2$	3×10^{-5}	E, T_{in}, ms	[32]
$Cd(NO_3)_2$	590	$CdO(s) + 2NO_2 + 0.5O_2$	$CdO(g) + 2NO_2 + 0.5O_2$	1×10^{-6}	E, T_{in}, ms	[32]
NiC_2O_4	570	$Ni(s) + 2CO_2$	$Ni(g) + CO + CO_2 + 0.5O_2$	1×10^{-17}	E, T_{in}	[47]
$Ag_2C_2O_4$	370	$2Ag(s) + 2CO_2$	$2Ag(g) + CO + CO_2 + 0.5O_2$	7×10^{-38}	E, T_{in}	[47]
$Pb(N_3)_2$	500	$Pb(s) + 3N_2$	$Pb(g) + N + N_2 + N_3$	2×10^{-34}	E, T_{in}, J	[74]
$Ba(N_3)_2$	390	$Ba(s) + 3N_2$	$Ba(g) + 0.6N + 2.7N_2$	8×10^{-16}	E, T_{in}, J	[74]
TlN_3	400	$Tl(s) + 1.5N_2$	$Tl(g) + N + N_2$	3×10^{-40}	E, T_{in}, ms	[74]

[a] The ms is mass-spectrometry analysis.

whereas the induction period at 400 K takes more than 50 min.

The difference between the primary products for the equilibrium and deduced reactions consists, firstly, in the different phases of metal or metal oxide species (solid and gas, respectively) and, secondly, in the different composition of gaseous components (only for oxalates and azides). As a result of this 'double distinction' in the overall composition of primary products, the vaporization coefficients for oxalates and azides are much lower (10^{-15}–10^{-40}) than those for nitrates (10^{-5}–10^{-7}). This explains the thermal stability of these explosive compounds at room temperature. As before, the discrepancy between the experimental and theoretical values in most cases was not more than 10% for the E and T_{in} parameters and a factor of three for the J parameter.

4.3.4. Solids decomposed into gaseous and solid products (taking into account the condensation energy transfer to the reactant)

This class of decompositions is of prime interest for traditional studies into crystolysis reactions. A peculiarity of these reactions is the formation of the interface zone between reactant and product when, due to the condensation energy transfer to the reactant, the rate of reaction reaches the steady state.

Table 11 presents a list of reactants which have had their decomposition investigated. The choice of compounds for the investigation has been defined by the availability in the literature of reliable experimental data on the kinetics of decomposition and thermodynamic functions for the components of reactions. The composition of the primary products for deduced reactions corresponds, as before, to the best agreement between experimental and calculated values of both kinetic parameters: E and one of the additional P, k, J, A or T_{in} parameters. The discrepancy between experiment and theory is not more than 10% for the E and T_{in} parameters and a factor of three for the P, k, J and A parameters.

In agreement with the theoretical assumptions (Section 2.1), the value of the τ parameter (defining a part of the condensation energy consumed by the reactant) in all cases, except $Mg(OH)_2$ and $Li_2SO_4{\cdot}H_2O$, was taken to be 0.5. For the last two compounds, which are decomposed with the formation of H_2O as one of the primary products, $\tau \cong 0.6$. We have no explanation for this difference. This fact is worthy of more careful consideration.

As before (Section 4.3.3), the lowest values of the vaporization coefficient (10^{-10}–10^{-23}) were observed for metal oxalates. In these cases, the difference in the composition of the primary products for equilibrium and deduced reactions is more significant than for other compounds. The most unexpected results here are the values of the α_v parameter for the oxides of Fe, Ni, Co and Cu (Table 11). In contrast to the α_v values for all other compounds, they are higher than unit (!) and are as high as 10^8–10^9. How is it possible that the decomposition into products different from those at equilibrium occurs faster than that into the equilibrium products?

Table 11
Thermal decomposition of inorganic compounds into gaseous and solid products ($\tau = 0.5$ for all compounds except $Mg(OH)_2$ and $Li_2SO_4{\cdot}H_2O$ for which $\tau = 0.6$)

Reactant	T (K)	Primary products		α_v	Experimental parameters[a]	Reference
		Equilibrium	Deduced			
Ag_2O	600	$2Ag(s) + 0.5O_2$	$2Ag(g)_\downarrow + 0.5O_2$	5×10^{-7}	E, k	[79]
FeO	1270	$Fe(s) + 0.5O_2$	$Fe(g)_\downarrow + 0.5O_2$	2×10^{9}	E^b, T_{in}	[80]
NiO	950	$Ni(s) + 0.5O_2$	$Ni(g)_\downarrow + 0.5O_2$	4×10^{8}	E, T_{in}	[80]
CoO	1100	$Co(s) + 0.5O_2$	$Co(g)_\downarrow + 0.5O_2$	2×10^{8}	E, T_{in}	[80]
Cu_2O	900	$2Cu(s) + 0.5O_2$	$2Cu(g)_\downarrow + 0.5O_2$	4×10^{7}	E, T_{in}	[80]
GaN	1000	$Ga(s) + 0.5N_2$	$Ga(g)_\downarrow + 0.5N + 0.25N_2$	3×10^{-6}	E, P	[73]
$Mg(OH)_2$	550	$MgO(s) + H_2O$	$MgO(g)_\downarrow + H_2O$	4×10^{-5}	E^b, J	[81]
$MgSO_4$	1150	$MgO(s) + SO_2 + 0.5O_2$	$MgO(g)_\downarrow + SO_2 + O$	4×10^{-4}	E, T_{in}	[21]
NiC_2O_4	570	$Ni(s) + 2CO_2$	$Ni(g)_\downarrow + CO + CO_2 + 0.5O_2$	5×10^{-12}	E, T_{in}, re	[47]
MnC_2O_4	660	$MnO(s) + CO_2 + CO$	$MnO(g)_\downarrow + 2CO + 0.5O_2$	3×10^{-10}	E, T_{in}	[47]
$Ag_2C_2O_4$	370	$2Ag(s) + 2CO_2$	$2Ag(g)_\downarrow + CO + CO_2 + 0.5O_2$	1×10^{-23}	E, T_{in}, re	[47]
PbC_2O_4	540	$PbO(s) + CO_2 + CO$	$PbO(g)_\downarrow + 2CO + 0.5O_2$	2×10^{-9}	E, T_{in}	[47]
$Li_2SO_4{\cdot}H_2O$	320	$Li_2SO_4(s) + H_2O$	$Li_2SO_4(g)_\downarrow + H_2O$	1×10^{-4}	E^b, A	[82]
$MgCO_3$	780	$MgO(s) + CO_2$	$MgO(g)_\downarrow + CO_2$	4×10^{-8}	E, k	[75]
$CaCO_3$	970	$CaO(s) + CO_2$	$CaO(g)_\downarrow + CO_2$	1×10^{-4}	E, J	[75]
$SrCO_3$	980	$SrO(s) + CO_2$	$SrO(g)_\downarrow + CO_2$	4×10^{-2}	E, k	[75]
Pb_3O_4	800	$3PbO(s) + 0.5O_2$	$3PbO(g)_\downarrow + O$	1×10^{-2}	E, T_{in}, ind	[75]
Fe_4N	620	$4Fe(s) + 0.5N_2$	$4Fe(g)_\downarrow + 0.5N_2$	1×10^{-12}	E, T_{in}	[75]
$FeCl_3$	410	$FeCl_2(s) + 0.5Cl_2$	$FeCl_2(g)_\downarrow + 0.5Cl_2$	2×10^{-6}	E, T_{in}	[75]
$LiCl{\cdot}H_2O$	330	$LiCl(s) + H_2O$	$LiCl(g)_\downarrow + H_2O$	2×10^{-4}	E, T_{in}	[75]

[a] Here re: the retardation effect; ind: the indirect observation of atomic oxygen.
[b] In isobaric and equimolar modes.

The reason of this phenomenon lies, firstly, in a higher rate of reaction $MO(s) \rightarrow M(g) + 0.5O_2$ in comparison with that of reaction $MO(s) \rightarrow M(s) + 0.5O_2$, and secondly, in a higher rate of reaction $MO(s) \rightarrow M(g)_\downarrow + 0.5O_2$ (at $\tau = 0.5$) in comparison with that of reaction $MO(s) \rightarrow M(g) + 0.5O_2$ (at $\tau = 0$). Such behavior can occur only for a few metal oxide-free metal combinations that meet some thermodynamic requirements. To understand this, let us consider the relationship which follows from Eq. (11) for the α_v parameter:

$$\alpha_v = \frac{P_d}{P_e} \cong \frac{(F^{1/\nu})_e}{(F^{1/\nu})_d} \frac{\exp(\Delta S^\circ_T/\nu R)_d}{\exp(\Delta S^\circ_T/\nu R)_e} \frac{\exp(-\Delta_r H^\circ_T/\nu RT)_d}{\exp(-\Delta_r H^\circ_T/\nu RT)_e} \tag{31}$$

The factors related to deduced and equilibrium reactions are marked with letters d and e, respectively. For simplicity, we neglect here the factors connected with the different molar masses of the products. If we further neglect the distinction of the two first factors from unity (their product is in the range 1/3–3), we obtain

$$\alpha_v \cong \exp \frac{1}{RT} \left[\left(\frac{\Delta_r H^\circ_T}{\nu} \right)_e - \left(\frac{\Delta_r H^\circ_T}{\nu} \right)_d \right] \tag{32}$$

To satisfy the condition $\alpha_v \geq 1$, it is necessary that

$$\left(\frac{\Delta_r H^\circ_T}{\nu} \right)_e \geq \left(\frac{\Delta_r H^\circ_T}{\nu} \right)_d \tag{33}$$

For a metal oxide of the type MO at 298 K, condition (33) is equivalent to

$$\frac{-\Delta H^\circ_{298}(MO)}{0.5} \geq \frac{0.5\Delta H^\circ_{298}(M) - \Delta H^\circ_{298}(MO)}{1.5}$$

or

$$\Delta H^\circ_{298}(M) \leq -4\Delta H^\circ_{298}(MO) \tag{34}$$

where $\Delta H^\circ_{298}(M)$ and $\Delta H^\circ_{298}(MO)$ are the enthalpies of formation of gaseous M and solid MO at 298 K.

Moreover, in the case of condensation of gaseous metal, the condition $T_{in}(1) > T_{in}(2)$ should be met

where the initial temperatures $T_{in}(1)$ and $T_{in}(2)$ correspond, respectively, for the reactions: $M(s) \rightarrow M(g)$ and $MO(s) \rightarrow M(g)_{\downarrow} + 0.5O_2$. If we take into account that $T_{in} \propto E$ (see Sections 2.2.3 and 4.4), we find that

$$\Delta H^{\circ}_{298}(M) \geq \frac{-\Delta H^{\circ}_{298}(MO) + 0.5\Delta H^{\circ}_{298}(M)}{1.5}$$

or

$$\Delta H^{\circ}_{298}(M) \geq -\Delta H^{\circ}_{298}(MO) \quad (35)$$

Therefore, to satisfy the condition $\alpha_v \geq 1$ for metal oxides of the type MO, it is necessary that

$$-\Delta H^{\circ}_{298}(MO) \leq \Delta H^{\circ}_{298}(M) \leq -4\Delta H^{\circ}_{298}(MO) \quad (36)$$

In a similar way, for metal oxides of the type M_2O, it is possible to obtain

$$-\tfrac{2}{3}\Delta H^{\circ}_{298}(MO) \leq \Delta H^{\circ}_{298}(M) \leq -4\Delta H^{\circ}_{298}(MO) \quad (37)$$

As can be seen from Table 12, for many oxides of the type MO and M_2O, conditions (36) and (37) are fulfilled only for FeO, CoO, NiO and PdO in the first case and only for Cu_2O, in the second. For other oxides, condition (35) or, as for Ag_2O, condition (34) are not met.

The identification of the dissociative evaporation mechanism of thermal decomposition for this selected group of oxides allowed us to reconsider the traditional views on the mechanism of reduction of these oxides by carbon [80]. Contrary to the accepted concepts, the function of carbon in this process is to react with the oxygen liberated from the decomposition of the oxide, thus maintaining a low partial pressure of oxygen (the equimolar mode of decomposition) in the furnace. In another words, carbon fulfills the role of buffer in this process.

4.4. Desorption of sub-nanogram masses of elements from graphite and platinum group metals

Hitherto, we have considered applications of the physical approach to investigations of the mechanisms and kinetics of sublimation/decomposition processes. However, the potentialities of this approach are not limited to these applications. There are some other heterogeneous processes in which the use of this physical approach might be helpful, in particular, heterogeneous catalysis and the interactions of solids with gases and metal vapors. We shall consider below some results of applications of the physical approach to the investigation of the mechanism of analyte release in ET AAS. This technique is based on the fast evaporation of a sample in a small graphite tube and measurement of the absorpion of the light beam passed through this tube by free atoms of analyte. To achieve more efficient separation of the analyte and the matrix during a preliminary pyrolysis stage, 1–10 μg of one of the platinum group metals (most frequently, palladium) as its nitrate solution is added to each sample as a chemical matrix modifier.

The interpretation of the mechanism of release of sub-nanogram masses of analytes from graphite and platinum group modifiers (PGM) is one of the oldest and, up to now, one of the most controversial problems in ET AAS. From the very first investigations in the 1970s, two main approaches have been defined. By the

Table 12
Values of enthalpy for the formation of some gaseous metals and solid metal oxides at 298 K [83]

Oxide	$-\Delta H^{\circ}_{298}(MO)$ (kJ mol^{-1})	$\Delta H^{\circ}_{298}(M)$ (kJ mol^{-1})	$-4\Delta H^{\circ}_{298}(MO)$ (kJ mol^{-1})
FeO	264.8	417.0	1059.4
CoO	238.9	428.4	955.6
NiO	239.7	428.8	959.0
PdO	115.5	372.3	461.9
CdO	259.0	111.8	1036.0
MnO	384.9	384.5	1539.7
PbO	218.6	195.2	914.6
MgO	601.5	147.1	2406.0
Cu_2O	115.5[a]	337.6	692.7
Ag_2O	20.8[a]	284.9	124.5

[a] These values correspond to $-(2/3)\Delta H^{\circ}_{298}(MO)$.

first approach, called adsorption/desorption (A/D), the analyte at the instant of entering the gas phase is assumed to be distributed in a monolayer over the furnace surface, or in the form of individual atoms or molecules bound to the surface by physi- or chemisorption forces. By the second approach involving condensation/evaporation (C/E) processes, the original samples, just as the possible products of condensation, are assumed to be distributed in microcrystallites or microdroplets possessing thermochemical characteristics typical for bulk amounts of these substances.

Over the past two decades, many studies have been performed in this area. In most of these studies, the Arrhenius plots that characterize the vaporization rate constants were used for the determination of (so-called) activation energies, E. These values were compared with enthalpy changes, $\Delta_r H^\circ_T$, for suspected release reactions. But no consensus has developed as to the most likely mechanisms of atom formation. As an illustration, two examples can be given.

Sturgeon and Arlow [84], based on the results of an investigation of 3–30 ng Pb, Bi and Au atomization from a graphite surface at atmospheric pressure and in vacuum, concluded that "Arrhenius data support a vaporization model that assumes the analyte to be present on the graphite surface in the form of microparticles as opposed to a monolayer". However, in the subsequent study [85] performed in the same laboratory for 0.7–23 ng Pb, the average E parameter measured (205 ± 25 kJ mol^{-1}) was only half of that (400 ± 20 kJ mol^{-1}) found in [84]. Moreover, an apparent first-order rate of Pb release typical for a monolayer distribution was observed. The authors [85] interpreted this last value of E as a desorption energy of Pb from a monolayer film, in contrast to the former value correlated with the enthalpy of PbO dissociative evaporation. The difference in the mechanism of release in both experiments was attributed to the presence of nitric acid in samples in [84] and not in [85].

Still more controversy is evident in the interpretation of the mechanism of atomization of copper. Two different release modes have been implicated in low temperature and high temperature regions with different values of the E parameter (310–340 and 130–190 kJ mol^{-1}, respectively). The first value is interpreted as the enthalpy of evaporation of bulk metal. The low value of E was associated with the dissociation of Cu_2 molecules [86], with the formation of copper acetylide Cu_2C_2 [87] and with the diffusional-kinetic regime of evaporation of the bulk metal from porous graphite [88]. In 1987, McNally and Holcombe [89] concluded that Cu desorbs from the graphite surface as individual atoms. This conclusion was based on the observation of a first-order release of 0.06–2 ng Cu and a low value of the E parameter (124 ± 10 kJ mol^{-1}). These experiments were repeated later in the same laboratory by Fonseca et al. [90]. For 0.24 ng of Cu, the E parameter was found to be 176 ± 20 kJ mol^{-1}. Lynch et al. [85] generally supported these observations, namely, a first-order release and the low value (146 ± 20 kJ mol^{-1}) of E parameter (for 0.15–1 ng of Cu). At the same time, as the sample mass was increased beyond 2 ng, the E value increased to 188–209 kJ mol^{-1} [85].

In contrast with the above interpretation, L'vov et al. [91,92] subsequently attempted to explain these features of Cu release from graphite in the framework of the C/E approach. In particular, these authors [92] pointed out that the low E parameter observed can be interpreted as that for the reduction of CuO by carbon (190 kJ mol^{-1}).

The solution of this stubborn problem of the correct interpretation of the release mechanism turned out to be totally unexpected. Unfortunately, during the long time when we had used a physical approach in the analysis of decomposition mechanisms, we paid no attention to the possibility of applying the same approach to the analysis of the desorption mechanism of release. Recall, that one of the consequences of this approach is theoretical relationship (23):

$$\frac{T_{app}}{E} \cong \frac{1}{\Delta S^\circ_T/\nu - R \ln P_{app}}$$

between the initial/appearance temperature and E parameter. For gasification (sublimation or dissociative evaporation) of 1 mol of solid (metal or compound), the average value of $\Delta S^\circ_T(E) \equiv \Delta S^\circ_T/\nu = 140 \pm 20$ J mol^{-1} K^{-1}. If we take into account that the appearance temperature, T_{app}, in ET AAS corresponds approximately to $P_{app} = 10^{-7}$ atm [93], we obtain $T_{app}/E \cong 3.6 \pm 0.2$ K mol kJ^{-1}.

In the case of desorption of metal atoms ($\nu = 1$), present on the surface as a monatomic two-dimensional gas, the average value ΔS°_T(D) should be much smaller, because it corresponds to an atom transfer

from a two-dimensional to a three-dimensional gas. These states differ only in their statistical sums (partition functions) for the translational movement of atoms and the difference in entropy can be estimated from statistical mechanics as [94]

$$\Delta S^{\circ}_{T}(D) = \frac{R(2.5 \ln T + 1.5 \ln M - 1.16487)}{3} \qquad (38)$$

The mean value of $\Delta S^{\circ}_{T}(D)$ for desorption of metal atoms with the mean molar mass, $M = 0.05$ kg mol^{-1}, at $T = 1500$ K equals 35 J mol^{-1} K^{-1}. Therefore, in the case of desorption of metal atoms, the mean ratio $T_{app}/E \cong 5.9$ K mol kJ^{-1}, i.e. 1.6 times larger than that for their evaporation/decomposition from the bulk.

The large difference in ΔS°_{T} values for these processes manifests itself also in the values of pre-exponential factors, A, typical for these processes. It follows from the theory that the ratio

$$\frac{A(E)}{A(D)} = \exp\left(\frac{\Delta S^{\circ}_{T}(E) - \Delta S^{\circ}_{T}(D)}{R}\right) \cong 3 \times 10^{5} \qquad (39)$$

Thus, instead of the averaged value $A(E) \cong 3 \times 10^{11}$ s^{-1} for the large group of elements [20], the value $A(D)$ should correspond to about 10^{6} s^{-1}. The use of these criteria (T_{app}/E ratio and A value) in the analysis of experimental data allows the true mechanism of release to be identified from the two versions.

In our recent work [93], we used this method for the identification of the mechanism of analyte retention on a palladium modifier. The experimental values of T_{app}/E for the release of Ag, As, Au, Bi, Cd, Cu, Se and Tl from a palladium modifier were compared with the theoretical values (Table 13). The average values (for all analytes) of T_{app}/E are found to be in excellent agreement: 5.8 ± 0.5 (experimental) and 5.8 ± 0.1 K mol kJ^{-1} (theoretical). It was concluded from this that the release of these analytes from solid palladium (the E parameters were measured at temperatures below the melting point of Pd) occurs via desorption of individual atoms and, as a consequence, their retention on palladium in the pyrolysis stage can be ascribed to the mechanism of dissociative chemisorption.

In continuation of the above study, we analyzed [100] the results of similar investigations into the mechanism of Se, Bi, Sn and Cr retention on other PGM: Pt, Rh and Ru. Deduced from the results, the averaged ratio of T_{app}/E for all 11 analyte-PGM combinations (5.9 ± 0.9 K mol kJ^{-1}) is in good agreement with theory. A rather high value for the standard deviation may be ascribed to errors in the determinations of both kinetic parameters and to a deviation of the P_{app} value from the mean (10^{-7} atm) because of the different sensitivity of AAS determination for different elements. Based on these and previous [93] results, we can state with confidence that the retention of analytes on all PGM can be ascribed to the mechanism of dissociative chemisorption.

To this end, we collected and analyzed critically the published kinetic parameters for the analyte release from graphite (Table 14). For all 13 analytes, $T_{app}/E = 6.6 \pm 0.9$ K mol kJ^{-1}. This result, within the accuracy of the analysis, is in agreement with the theoretical value for the desorption mechanism of release. Still more impressive is the agreement between theoretical and experimental values of pre-exponential factor, A, of the Arrhenius equation for the

Table 13
Experimental and theoretical values of T_{app}/E ratio for the analytes released from solid palladium

Analyte	Sample	T_{app} (K)	E (kJ mol^{-1})	ΔS°_{T} (J mol^{-1} K^{-1})	T_{app}/E (K mol kJ^{-1})		Reference
					Experiment	Theory	
Ag	In HNO_3	1778	338 ± 6	39.4	5.3	5.8	[96]
As	AsH_3	1693	303 ± 12	37.5	5.6	5.8	[95]
Au	In HNO_3	1508	274 ± 10	40.7	5.5	5.7	[97]
Bi	BiH_3	1380	251 ± 20	40.4	5.5	5.7	[95]
Cd	In HNO_3	1293	218 ± 3	37.8	6.3	5.8	[98]
Cu	In HNO_3	1250	192	34.7	6.5	5.9	[99]
Se	SeH_2	1465	247 ± 12	36.7	5.9	5.9	[95]
Tl	In HNO_3	1709	288 ± 3	41.7	5.9	5.7	[96]

Table 14
Kinetic parameters for the release of sub-nanogram masses of some analytes from graphite

Analyte	T_{app} (K)	E (kJ mol^{-1})	T_{app}/E (K mol kJ^{-1})	Reference
Ag	1000	159 ± 13	6.3	[85]
Au	1115	197 ± 8	5.7	[85]
Cd	890	120 ± 6	7.4	[102]
Co[a]	1500	285 ± 9	5.3	[103]
Cr	1670	253 ± 15	6.6	[101]
Cu	1270	172 ± 4	7.4	[104]
In[b]	900	142 ± 17	6.3	[105]
Mn	1480[c]	180 ± 25	8.2	[105]
Ni	1540	268 ± 4	5.7	[104]
Pb	1210	205 ± 25	5.9	[85]
Pd	1380[d]	184 ± 12	7.5	[105]
Ru	2170[d]	301 ± 15	7.2	[106]
Se	1500	240 ± 30	6.3	[107]

[a] Glassy carbon tube.
[b] For aerosol deposition.
[c] From Sturgeon et al. [86].
[d] From Sturgeon et al. [95].

release of copper from graphite. As mentioned above, this value should correspond in the case of desorption of individual atoms to 10^6 s^{-1}. Fonseca et al. [90] used exactly the same value of the A-factor when they simulated the process of copper release from graphite. This value corresponded to the best agreement between the simulated generation rate and the observed absorption signal.

5. Conclusions

In the first part of this work, it has been shown that the physical approach to the interpretation of the exponential dependence of the rate of heterogeneous (crystolysis) reactions on temperature proposed by Hertz and Langmuir and developed by the author, represents a rigorous self-consistent theory which is based on the reasonable assumptions and the formalism of the kinetic theory of gases and chemical thermodynamics. The second and third parts of this work were devoted to the application of this approach to the interpretation of some important features of crystolysis reactions and identification of the mechanisms of decomposition for several classes of solid reactants.

The most important results of this theoretical analysis, which supports the advantages of the physical approach over those of the more traditional chemical approach, may be formulated as follows.

1. The physical approach allows, for the first time, the *quantitative* interpretation of the following features of crystolysis reactions: the mechanism of nucleation and the source of energy supporting the autocatalytic development of decomposition reactions, the retardation of decomposition in the presence of gaseous products, the low vaporization coefficients for many substances and the thermal stability of some explosives at room temperature, the effect of self-cooling on the measurement of kinetic parameters, the Topley–Smith effect and the kinetic compensation effect.
3. The physical approach has been successfully applied to the interpretation of the kinetics of sublimation/dissociative evaporation of more than 110 substances from 20 different classes of solids: metals, non-metals, oxides, hydroxides, sulphides, selenides, tellurides, nitrides, azides, carbides, borides, fluorides, chlorides, bromides, iodides, carbonates, nitrates, sulphates, oxalates and hydrates.
4. The physical approach can be equally used in investigations of the kinetics and mechanisms of decompositions of all types of crystals: molecular, ionic, covalent and metallic.

5. The mechanism of dissociative evaporation provides an explanation for the enigmatic process of low-temperature (<1000°C) 'carbothermal reduction' of Fe, Co, Ni and Cu oxides.
6. The physical approach can be used in ET AAS and QMS investigations of the desorption mechanism of release of sub-nanogram masses of analytes from graphite and from metal surfaces.

It is necessary to admit in conclusion that the effect of activation (in terms of a commonly accepted model) in the case of crystolysis reactions is not more than an illusion. The application of the Arrhenius original approach (and later on, the Polanyi–Wigner and Eyring–Evans–Polanyi treatments) to the kinetics of solid decompositions was wrong, and it resulted in a stagnation of theory of crystolysis reactions over many years. It is hoped that the physical approach provides a real challenge to the future progress of crystolysis chemistry.

Acknowledgements

I thank Dr. Andrew Galwey for encouraging discussions during my recent visit to Belfast which stimulated me to write this paper and his fruitful comments on a draft of this manuscript.

References

[1] M.E. Brown, D. Dollimore, A.K. Galwey, Reaction in the Solid State, Elsevier, Amsterdam, 1980.
[2] A.K. Galwey, M.E. Brown, Thermal Decomposition of Ionic Solids, Elsevier, Amsterdam, 1999.
[3] A.K. Galwey, M.E. Brown, A theoretical justification for the application of the Arrhenius equation to kinetics of solid state reactions (mainly ionic crystals), Proc. R. Soc. London 450 (1995) 501–512.
[4] P.D. Garn, Kinetic parameters, J. Thermal Anal. 13 (1978) 581–593.
[5] R.D. Shannon, Activation complex theory applied to the thermal decomposition of solids, Trans. Faraday Soc. 60 (1964) 1902–1913.
[6] A.K. Galwey, Magnitudes of the Arrhenius parameters for decomposition reaction of solids, Thermochim. Acta 242 (1994) 259–264.
[7] A.K. Galwey, M.E. Brown, Solid-state decompositions — stagnation or progress? J. Thermal Anal. Cal. 60 (2000) 863–877.
[8] H. Hertz, Ueber die Verdunstung der Flüssigkeiten, insbesondere des Quecksilbers, im luftleeren Raume. II. Ueber den Druck des gesättigten Quecksilberdampfes, Ann. Phys. Chem. 17 (1882) 177–200.
[9] J.F. Dettorre, T.G. Knorr, E.H. Hall, Evaporation processes, in: C.F. Powel, J.H. Oxley, J.M. Blocher Jr. (Eds.), Vapor Deposition, Wiley, New York, 1966, pp. 62–101.
[10] I. Langmuir, The vapor pressure of metallic tungsten, Phys. Rev. 2 (1913) 329–342.
[11] I. Langmuir, The evaporation, condensation and reflection of molecules and the mechanism of adsorption, Phys. Rev. 8 (1916) 149–176.
[12] I. Langmuir, The evaporation of small spheres, Phys. Rev. 12 (1918) 368–370.
[13] G.A. Somorjai, J.E. Lester, Evaporation mechanism of solids, in: H. Reiss (Ed.), Progress in Solid State Chemistry, Pergamon Press, Oxford, 1967, pp. 1–51.
[14] A.W. Searcy, The kinetics of evaporation and condensation reactions, in: A.W. Searcy, D.V. Ragone, U. Colombo (Eds.), Chemical and Mechanical Behavior of Inorganic Materials, Wiley, New York, 1970 pp. 107–133.
[15] A.W. Searcy, D. Beruto, Transition state theory for vaporization and condensation, J. Phys. Chem. 78 (1974) 1298–1304.
[16] B.V. L'vov, G.N. Ryabchuk, Studies of the mechanisms of sample atomization in electrothermal atomic absorption spectrometry by analysis of absolute process rates. Oxygen-containing compounds, Zh. Anal. Khim. 36 (1981) 2085–2096 (in Russian).
[17] B.V. L'vov, G.H.A. Fernandes, Regularities in thermal dissociation of oxides in graphite furnaces for atomic absorption analysis, Zh. Anal. Khim. 39 (1984) 221–231 (in Russian).
[18] B.V. L'vov, The mechanism of thermal decomposition of metal nitrates in graphite furnaces for atomic absorption analysis, Zh. Anal. Khim. 45 (1990) 2144–2153 (in Russian).
[19] B.V. L'vov, Mechanism of the thermal decomposition of metal nitrates from graphite mass spectrometry studies, Mikrochim. Acta Wien 11 (1991) 299–308.
[20] B.V. L'vov, Interpretation of atomization mechanisms in electrothermal atomic absorption spectrometry by analysis of the absolute rates of the processes, Spectrochim. Acta B 52 (1997) 1–23.
[21] B.V. L'vov, Advances and problems in the investigation of the mechanisms of solid-state reactions by analysis of absolute reaction rates, Spectrochim. Acta B 53 (1998) 809–820.
[22] S. Arrhenius, Ueber die Reactiongeschwindigkeit bei der Inversion von Rohrzucker durch Säuren, Z. Phys. Chem. 4 (1889) 226–248 (a translation of the four pages in this paper that deal with temperature dependence is included in M.H. Back, K.J. Laidler (Eds.), Selected Readings in Chemical Kinetics, Pergamon Press, Oxford, 1967, pp. 31–35).
[23] B.V. L'vov, Mechanism and kinetics of carbothermal reduction of oxides, Izv. Vuzov. Chern. Metallurgiya 1 (1986) 4–9 (in Russian).

[24] R.E. Sturgeon, D.F. Mitchell, S.S. Berman, Atomization of lead in graphite furnace atomic absorption spectrometry, Anal. Chem. 55 (1983) 1059–1064.
[25] D.A. Bass, J.A. Holcombe, Mass spectral investigation of mechanisms of lead vaporization from a graphite furnace used in electrothermal atomizers, Anal. Chem. 59 (1987) 974–980.
[26] M.S. Dressler, J.A. Holcombe, Mass spectral and atomic absorption studies of selenium vaporization from a graphite surface, Spectrochim. Acta B 42 (1987) 981–994.
[27] N.S. Ham, T. McAllister, Graphite furnace mass spectrometry of cobalt, Spectrochim. Acta B 43 (1988) 789–797.
[28] P. Wang, V. Majidi, J.A. Holcombe, Copper atomization mechanisms in graphite furnace atomizers, Anal. Chem. 61 (1989) 2652–2658.
[29] D.C. Hassell, V. Majidi, J.A. Holcombe, Temperature programmed static secondary ion mass spectrometric study of phosphate chemical modifiers in electrothermal atomizers, J. Anal. Atom. Spectrom. 6 (1991) 105–108.
[30] L.J. Prell, D.L. Styris, D.A. Redfield, Comparison of atomization mechanisms for group IIA elements in electrothermal atomic absorption spectrometry, J. Anal. Atom. Spectrom. 5 (1991) 25–32.
[31] R.W. Fonseca, K.I. Wolfe, J.A. Holcombe, Mechanisms of vaporization for Cr using electrothermal atomization, Spectrochim. Acta B 49 (1994) 411–429.
[32] B.V. L'vov, A.V. Novichikhin, Mechanism of thermal decomposition of anhydrous metal nitrates, Spectrochim. Acta B 50 (1995) 1427–1448.
[33] B.V. L'vov, A.V. Novichikhin, Mechanism of thermal decomposition of hydrated copper nitrate in vacuo, Spectrochim. Acta B 50 (1995) 1459–1468.
[34] D.L. Styris, D.A. Redfield, Mechanisms of graphite furnace atomization of aluminium by molecular beam sampling mass spectrometry, Anal. Chem. 59 (1987) 2891–2897.
[35] B. McCarroll, G. Ehrlich, Condensation and energy transfer on crystals: in: E. Rutner, P. Goldfinger, J.P. Hirth (Eds.), Condensation and Evaporation of Solids, Gordon and Breach, New York, 1964, pp. 521–538.
[36] B.V. L'vov, Mechanism of thermal decomposition of alkaline-earth carbonates, Thermochim. Acta 303 (1997) 161–170.
[37] J.P. Hirth, G.M. Pound, Condensation and Evaporation. Nucleation and Growth Kinetics, Pergamon Press, Oxford, 1963.
[38] J.M. Criado, M. Gonzalez, J. Malek, A. Ortega, The effect of the CO_2 pressure on the thermal decomposition kinetics of calcium carbonate, Thermochim. Acta 254 (1995) 121.
[39] D. Dollimore, T.A. Evans, Y.F. Lee, F.W. Wilburn, Correlation between the shape of a TG/DTG curve and the form of the kinetic mechanism which is applying, Thermochim. Acta 198 (1992) 249–257.
[40] M.M. Pavlyuchenko, V.V. Samuskevich, E.A. Prodan, Effect of water vapor on the dehydration of $La_2(CO_3)_3{\cdot}8H_2O$, Vesti AN BSSR, Ser. Khim. 6 (1970) 11–15 (in Russian).
[41] M.C. Ball, L. Portwood, The dehydration of copper (II) acetate monohydrate, J. Thermal Anal. 41 (1994) 347–356.
[42] V.V. Samuskevich, E.A. Prodan, I.V. Kluy, The dehydration kinetics of $MnHPO_4{\cdot}3H_2O$, Vesti AN BSSR, Ser. Khim. 1 (1984) 47–51 (in Russian).
[43] M.M. Pavlyuchenko, V.V. Kokhanovskii, E.A. Prodan, The dehydration kinetics $Y_2(CO_3)_3{\cdot}4H_2O$, in: M.M. Pavlyuchenko (Ed.), Heterogeneous Chemical Reactions, Nauka i Tekhnika, Minsk, 1970, pp. 168–190 (in Russian).
[44] E.A. Prodan, S.I. Pytlev, Surface dehydration of $Na_3P_3O_9{\cdot}6H_2O$ crystals, Zh. Fis. Khim. 57 (1983) 1998–2001 (in Russian).
[45] B.V. L'vov, A.V. Novichikhin, Quantitative interpretation of the evaporation coefficients for the decomposition or sublimation of some substances in vacuo, Thermochim. Acta 290 (1997) 239–251.
[46] B.V. L'vov, Kinetics and mechanism of thermal decomposition of mercuric oxide, Thermochim. Acta 333 (1999) 21–26.
[47] B.V. L'vov, Kinetics and mechanism of thermal decomposition of nickel, manganese, silver, mercury and lead oxalates, Thermochim. Acta 364 (12) (2000) 99–109.
[48] J.Y. Macdonald, The thermal decomposition of silver oxalate, J. Chem. Soc. (1936) 832–847.
[49] D. Dollimore, T.A. Evans, The thermal decomposition of oxalates. Part 23. An isothermal kinetic study into the effect of the environmental atmosphere on the thermal decomposition of silver oxalate, Thermochim. Acta 178 (1991) 263–271.
[50] E.G. Prout, F.C. Tompkins, The thermal decomposition of mercuric oxalate, Trans. Faraday Soc. 43 (1947) 148–157.
[51] M.L. Smith, B. Topley, The experimental study of the rate of dissociation of salt hydrates, Proc. R. Soc. A 134 (1931) 224–245.
[52] B.V. L'vov, A.V. Novichikhin, A.O. Dyakov, Mechanism of thermal decomposition of magnesium hydroxide, Thermochim. Acta 315 (1998) 135–143.
[53] B.V. L'vov, A.V. Novichikhin, A.O. Dyakov, Computer simulation of the Topley–Smith effect, Thermochim. Acta 315 (1998) 169–179.
[54] J. Zawadzki, S. Bretsznajder, Ueber das Temperaturinkrement der Reaktionsgeschwindigkeit bei Reaktionen von Typus $A_{fest} = B_{fest} + C_{gas}$, Z. Electrochem. 41 (1935) 215–223.
[55] A.K. Galwey, M.E. Brown, Arrhenius parameters and compensation behaviour in solid-state decompositions, Thermochim. Acta 300 (1997) 107–115.
[56] J. Drowart, G. DeMaria, R.P. Burns, M.G. Inghram, Thermodynamic study of Al_2O_3 using a mass spectrometer, J. Chem. Phys. 32 (1960) 1366–1372.
[57] H.A. Jones, I. Langmuir, G.M.J. Mackay, The rates of evaporation and the vapor pressures of tungsten, molybdenum, platinum, nickel, iron, copper and silver, Phys. Rev. 30 (1927) 201–214.
[58] B. Paul, Compilation of evaporation coefficients, J. Am. Rocket Soc. (1962) 1321–1328.
[59] J. Vreštál, J. Kucera, Vapor pressure and thermodynamic study of the Co–Ni system, Metal Trans. 2 (1971) 3367–3372.

[60] B.V. L'vov, Mechanism of action of a palladium modifier, Spectrochim. Acta B 55 (2000) 1659–1668.
[61] An.N. Nesmeyanov, Vapor Pressure of Chemical Elements, AN SSSR, Moscow, 1961 (in Russian).
[62] R.C. Paule, Mass spectrometric studies of Al_2O_3 vaporization processes, High Temp. Sci. 8 (1976) 257–266.
[63] M. Greenbaum, J.N. Foster, M.L. Arin, M. Farber, The thermodynamic and physical properties of beryllium compounds. I. Enthalpy and entropy of vaporization of beryllium fluoride, J. Phys. Chem. 67 (1963) 36–40.
[64] D.A. Schulz, A.W. Searcy, Vapor pressure and heat of sublimation of calcium fluoride, J. Phys. Chem. 67 (1963) 103–106.
[65] I.G.F. Gilbert, J.A. Kitchener, The dissociation pressure of cadmium oxide, J. Chem. Soc. (1956) 3919–3921.
[66] M.A. Greenbaum, H.C. Ko, M. Wong, M. Farber, The vapor pressure and heat and entropy of sublimation of solid magnesium fluoride, J. Phys. Chem. 68 (1964) 965–968.
[67] R.G. Bautista, J.L. Margrave, Langmuir studies of the sublimation of strontium fluoride and barium fluoride single crystals, J. Phys. Chem. 69 (1965) 1770–1771.
[68] E.G. Wolff, C.B. Alcock, The volatilization of high-temperature materials in vacuo, Trans. Br. Ceram. Soc. 61 (1962) 667–687.
[69] An.N. Nesmeyanov, L.P. Firsova, E.P. Isakova, Determination of the saturated pressure of lead oxide, Zh. Fiz. Khim. 34 (1960) 1200–1204 (in Russian).
[70] L. Brewer, J. Kane, The importance of complex gaseous molecules in high temperature systems, J. Phys. Chem. 59 (1955) 105–109.
[71] R. Burns, Systematics of evaporation coefficient Al_2O_3, Ga_2O_3, In_2O_3, J. Chem. Phys. 44 (1966) 3307–3319.
[72] R.C. Paule, Mass spectrometric studies of Al_2O_3 vaporization processes, High Temp. Sci. 8 (1976) 257–266.
[73] B.V. L'vov, Kinetics and mechanism of thermal decomposition of GaN, Thermochim. Acta 360 (1) (2000) 85–91.
[74] B.V. L'vov, Mechanism of thermal decomposition of metal azides, Thermochim. Acta 291 (1997) 179–185.
[75] B.V. L'vov, unpublished data.
[76] H.W. Melville, S.C. Gray, The vapor pressure of red phosphorus, Trans. Faraday Soc. 32 (1936) 1026–1030.
[77] G.M. Rosenblatt, P.-K. Lee, M.B. Dowell, Vaporization of solids. Mechanism of retarded vaporization from a one-component single crystal, J. Chem. Phys. 45 (1966) 3454–3455.
[78] J.R. Soulen, P. Sthapitanonda, J. Margrave, Vaporization of inorganic substances: B_2O_3, TeO_2 and Mg_3N_2, J. Phys. Chem. 59 (1955) 132–136.
[79] B.V. L'vov, Kinetics and mechanism of thermal decomposition of silver oxide, Thermochim. Acta 333 (1999) 13–19.
[80] B.V. L'vov, Mechanism of carbothermal reduction of iron, cobalt, nickel and copper oxides, Thermochim. Acta 360 (2) (2000) 109–120.
[81] B.V. L'vov, A.V. Novichikhin, A.O. Dyakov, Mechanism of thermal decomposition of magnesium hydroxide, Thermochim. Acta 315 (1998) 135–143.
[82] B.V. L'vov, Mechanism of thermal decomposition of $Li_2SO_4{\cdot}H_2O$, Thermochim. Acta 315 (1998) 145–157.
[83] V.P. Glushko (Ed.), Thermodynamic Constants of Substances, Akademia Nauk SSSR, Moscow, 1962–1982 (in Russian).
[84] R.E. Sturgeon J.S. Arlow, Atomization in graphite furnace atomic absorption spectrometry: atmospheric pressure vis-a-vis vacuum vaporization. J. Anal. Atom. Spectrom, 1 (1986) 359–363 (in Russian).
[85] S. Lynch, R.E. Sturgeon, V.T. Luong, D. Littlejohn, Comparison of the energetics of desorption of solution and vapour phase deposited analytes in graphite furnace atomic absorption spectrometry, J. Anal. Atom. Spectrom. 5 (1990) 311–319.
[86] R.E. Sturgeon, C.L. Chakrabarti, C.H. Langford, Studies of the mechanisms of atom formation in graphite furnace atomic absorption spectrometry, Anal. Chem. 48 (1976) 1792–1807.
[87] D.A. Katskov, I.L. Greenstein, Investigation of chemical interaction of Cu, Au and Ag with carbon by atomic absorption method with electrothermal atomizers, Zh. Prikl. Spektrosk. 30 (1979) 787–792 (in Russia).
[88] B.V. L'vov, P.A. Bayunov, G.N. Ryabchuk, Macrokinetic theory of sample vaporization in electrothermal atomic absorption spectrometry, Spectrochim. Acta B 36 (1981) 397–425.
[89] J. McNally, J.A. Holcombe, Existence of microdroplets and dispersed atoms on the graphite surface in electrothermal atomizers, Anal. Chem. 59 (1987) 1105–1112.
[90] R.W. Fonseca, O.A. Guell, J. Holcombe, Electrothermal atomization of copper from graphite and tantalum surfaces, Spectrochim. Acta B 45 (1990) 1257–1264.
[91] B.V. L'vov, V.G. Nikolaev, A.V. Novichikhin, L.K. Polzik, Effect of platform material on sample vaporization rate in graphite furnace atomic absorption spectrometry, Spectrochim. Acta B 43 (1988) 1141–1146.
[92] B.V. L'vov, A.V. Novichikhin, L.K. Polzik, Critical comments on the application of the adsorption/desorption concept in graphite furnace atomic absorption spectrometry, Spectrochim. Acta B 47 (1992) 289–296.
[93] B.V. L'vov, Mechanism of action of a palladium modifier, Spectrochim. Acta B 55 (2000) 1659–1668.
[94] L.V. Gurvich, I.V. Veits, V.A. Medvedev, et al., Thermodynamic Properties of Individual Substances, Vol. 1, Nauka, Moscow, 1978, p. 28 (in Russian).
[95] R.E. Sturgeon, S.N. Willie, G.I. Sproule, P.T. Robinson, S.S. Berman, Sequestration of volatile element hydrides by platinum group elements for graphite furnace atomic absorption, Spectrochim. Acta B 44 (1989) 667–682.
[96] Y.-Z. Liang, Z.-M. Ni, Atom release of Mn, Co, Ag and Tl in a graphite furnace atomizer with and without palladium modifier, Spectrochim. Acta B 49 (1994) 229–241.
[97] N.S. Thomaidis, E.A. Piperaki, Determination of the kinetics parameters for the electrothermal atomization of gold with and without chemical modifiers, Spectrochim. Acta B 54 (1999) 1303–1320.
[98] M.A. Alvarez, N. Carrion, H. Gutierrez, Effects of atomization surfaces and modifiers on the electrothermal atomization of cadmium, Spectrochim. Acta B 50 (1995) 1581–1594.

[99] D. Rojas, M.A. Sanchez, W. Olivares, Influence of vapor redeposition and modifiers on the Arrhenius plots of copper in graphite furnace atomic absorption spectrometry, Spectrochim. Acta B 52 (1997) 1269–1281.
[100] B.V. L'vov, Method of absolute reaction rates supports the desorption mechanism of release of sub-nanogram masses of analytes from graphite and platinum group modifier surfaces, Spectrochim. Acta B 55 (2000) 1913–1919.
[101] R.N.S. Thomaidis, E.A. Piperaki, Effect of chemical modifiers on the kinetic parameters characterizing the electrothermal atomization of chromium, Spectrochim. Acta B 55 (2000) 611–627.
[102] M.A. Alvarez, N. Carrion, H. Gutierrez, Effect of atomization surfaces and modifiers on the electrothermal atomization of cadmium, Spectrochim. Acta B 50 (1995) 1581–1594.
[103] C.L. Chakrabarti, S.J. Cathum, Mechanism of cobalt atomization from different atomizer surfaces in graphite–furnace atomic absorption spectrometry, Talanta 37 (1990) 1111–1117.
[104] A.E. Bozdogan, A method for the determination of the kinetic parameters relevant to atom formation processes in electrothermal atomic absorption spectrometry, Spectrochim. Acta B 54 (1999) 557–569.
[105] J. McNally, J.A. Holcombe, Topology and vaporization characteristics of palladium, cobalt, manganese, indium and aluminum on a graphite surface using electrothermal atomic absorption, Anal. Chem. 63 (1991) 1918–1926.
[106] D. Rojas, W. Olivares, A method for the determination of the kinetic order and energy of the atom formation process in electrothermal atomization atomic absorption spectrometry, Spectrochim. Acta B 47 (1992) 387–397.
[107] J.L. Fisher, C.J. Rademeyer, Kinetics of selenium atomization in electrothermal atomization atomic absorption spectrometry, Spectrochim. Acta B 53 (1998) 537–548.